



Evaluation of the NSUF Reactor Activation and Damage (RAD) Calculator

March 2020

*Assessing the Accuracy of the Activation
Calculator*

Micah Gale

Nuclear Science User Facilities. Micah.Gale@inl.gov

Changing the World's Energy Future



DISCLAIMER

This information was prepared as an account of work sponsored by an agency of the U.S. Government. Neither the U.S. Government nor any agency thereof, nor any of their employees, makes any warranty, expressed or implied, or assumes any legal liability or responsibility for the accuracy, completeness, or usefulness, of any information, apparatus, product, or process disclosed, or represents that its use would not infringe privately owned rights. References herein to any specific commercial product, process, or service by trade name, trade mark, manufacturer, or otherwise, does not necessarily constitute or imply its endorsement, recommendation, or favoring by the U.S. Government or any agency thereof. The views and opinions of authors expressed herein do not necessarily state or reflect those of the U.S. Government or any agency thereof.

Evaluation of the NSUF Reactor Activation and Damage (RAD) Calculator

Determining the Accuracy of the Activation Calculator

Micah Gale
Nuclear Science User Facilities. Micah.Gale@inl.gov

March 2020

**Idaho National Laboratory
Nuclear Science User Facilities
Idaho Falls, Idaho 83415
<http://www.inl.gov>**

**Prepared for the
U.S. Department of Energy
Office of Nuclear Energy
Under DOE Idaho Operations Office
Contract DE-AC07-05ID14517**

Page intentionally left blank

ABSTRACT

Nuclear Science User Facilities developed an activation calculator as part of the Combined Material Experiment Toolbox project. The activation calculator estimates the radionuclide concentration in an irradiated sample to indicate when and where the samples may best be examined to only help with scoping the experiment. To verify the accuracy of the calculator, the results from the specific gamma dose rate [mrem/hr/g] at various cooldown times were compared to equivalent results generated in ORIGEN. Most elements were tested as a sample composed solely of that element. These samples were exposed to thirteen different lengths of irradiation in all reactor positions included in the calculator. For elements of interest (i.e., ones currently included in the Nuclear Fuels and Materials Library), 83% of the test cases fell within the allowed tolerance for this scoping tool of $\pm 50\%$. The overall error is logarithmic with irradiation length and is almost completely independent of reactor position. The primary source of error is missing nuclear data and reactions. NSUF believes that the RAD Calculator can be deployed to the user community because it is designed to provide estimates to aid researchers in planning experiments, and users are cautioned about the limitations of the calculator.

Page intentionally left blank

CONTENTS

1.	INTRODUCTION.....	1
2.	BACKGROUND.....	3
2.1	Theoretical Basis and Analytical Solution.....	3
2.2	Implemented Solution Method.....	4
2.2.1	Nuclear Data Resources.....	4
2.2.2	Building the Transmutation Matrices.....	4
2.2.3	Solving the Matrix Exponential with a Rational Approximation.	5
2.3	Acceptance Criterion.....	6
2.4	Reactor Power Levels Used	6
2.5	Potential Failure Modes	7
2.5.1	Time-Invariant Failure Modes	7
2.5.2	Time-Variant Failure Modes.....	7
3.	ANALYSIS.....	8
3.1	Benchmark Validation Against ORIGEN.....	8
3.1.1	Benchmark Validation for Elements of Interest Only.....	13
3.1.2	Out-of-Tolerance Elements.....	16
3.1.3	Convergence of the ORIGEN Solution.....	19
4.	RECOMMENDATIONS	20
4.1	Changes Needed Prior to Deployment.....	20
4.2	Medium-Term Changes (FY2020).....	20
4.2.1	Improving Nuclear Data.....	20
4.3	Long-Term Changes (FY2021).....	20
4.4	Other Calculator Modifications and Features to Consider.....	20
4.4.1	Calculator Assumptions	20
4.4.2	Implementation of Fuel Calculations.....	21
5.	REFERENCES.....	22

FIGURES

Figure 1.	The user input requesting the material to be irradiated and the desired amount of irradiation.....	1
Figure 2.	Example Output Showing Reactor Positions and Estimated Damage.....	2
Figure 3.	The specific activity of a material irradiated in a reactor position, based on user input.	2

Figure 4. Block diagram of how the RAD calculator works and the interactions between client and server.....	3
Figure 5. Core map for the ATR showing positions included in the calculator.....	9
Figure 6. Core map for the High Flux Isotope Reactor (HFIR).....	9
Figure 7. Core map for the Massachusetts Institute of Technology Reactor-II (MITR-II).....	10
Figure 8. Core map for North Carolina State University's PULSTAR Reactor.....	10
Figure 9. Accuracy of the RAD calculator when compared to ORIGEN based on simulated irradiation length.....	11
Figure 10 The accuracy of the RAD calculator compared to ORIGEN for specific gamma dose rate with respect to the simulated element irradiated.	12
Figure 11. Accuracy of the RAD calculator compared to ORIGEN for specific gamma dose rate with respect to the reactor position used.....	13
Figure 12. Accuracy of the RAD calculator, as compared to ORIGEN, for specific gamma dose rate with respect to the simulated element irradiated. Only materials in the NFML are included.	14
Figure 13. Accuracy of the RAD calculator, as compared to ORIGEN, for specific gamma dose rate with respect to the simulated irradiation length. Only materials in the NFML are included.	15
Figure 14. Accuracy of the RAD calculator, as compared to ORIGEN, for specific gamma dose rate with respect to the reactor position used. Only materials in the NFML are included.	15
Figure 15. Accuracy of the RAD calculator, as compared to ORIGEN, for specific gamma dose rate for iron with respect to the fast-to-total- flux ratio for each reactor position.	17
Figure 16. The relative difference between the RAD calculator and ORIGEN with respect to irradiation and cooldown time for iron in the MITR-ICSA position.....	18
Figure 17. The relative difference between the RAD calculator and ORIGEN with respect to irradiation and cooldown time for nickel in the MITR-ICSA position.	18

TABLES

Table 1 Power levels and operating cycles used by the calculator for the included reactors.	7
Table 2. Elements that, at least in one test case, fall outside the acceptable tolerance range.	16

Page intentionally left blank

ACRONYMS

Advanced Test Reactor (ATR)	4
Chebyshev Rational Approximation Method (CRAM)	4, 5
displacements per atom (DPA)	1
High Flux Isotope Reactor (HFIR)	9
Massachusetts Institute of Technology Reactor-II (MITR-II).	10
Nuclear Fuels and Materials Library (NFML).....	14
Nuclear Science User Facilities (NSUF)	1
ordinary differential equation (ODE).....	3
Reactor Activation and Damage (RAD) calculator	1

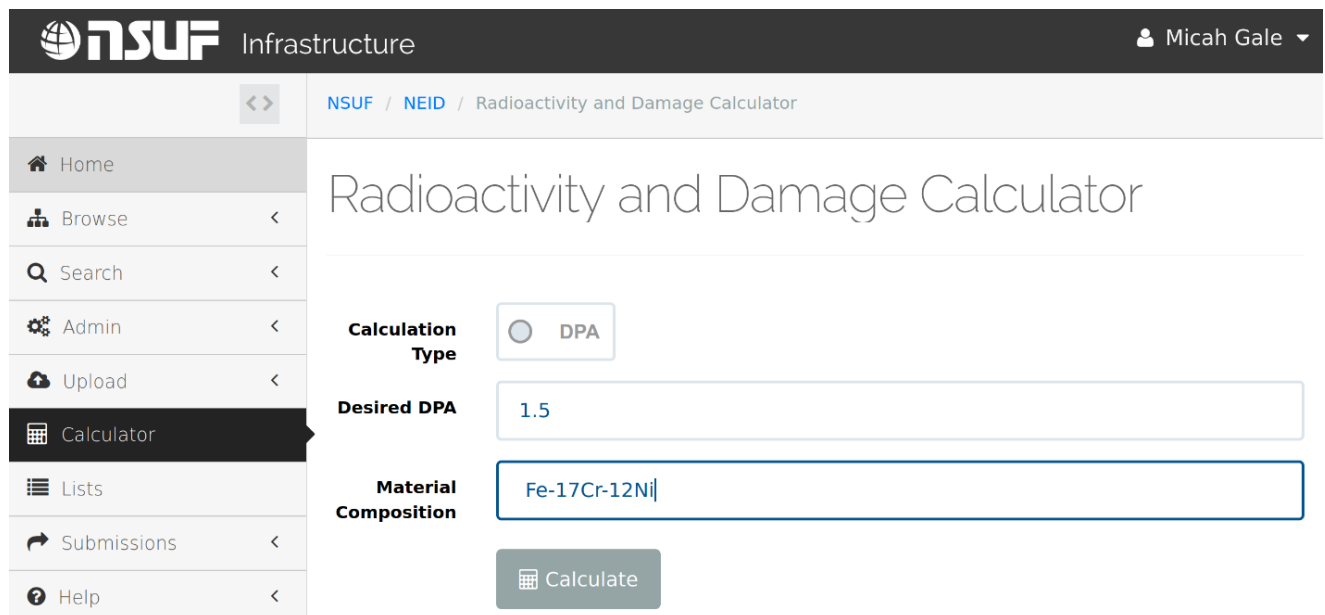
Page intentionally left blank

Evaluation of the NSUF Reactor Activation and Damage (RAD) Calculator

1. INTRODUCTION

The Reactor Activation and Damage (RAD) calculator was developed as part of the Combined Material Experiment Toolbox (CoMET) under the Nuclear Science User Facilities (NSUF) program. The RAD calculator estimates radiation damage [displacements per atom (DPA)] and activation accumulated during nominal irradiation at select NSUF reactors to aid researchers in planning and scoping their NSUF projects for the irradiation and post-irradiation-examination phase. This report focuses on the activation calculation process and does not cover damage calculations; damage is covered in report INL/EXT-20-58365 [1].

The calculator can be found at <https://nsuf-infrastructure.inl.gov/Calculator>. It starts by prompting the user for the material to be irradiated and the desired irradiation length or damage amount. Irradiation length is measured in effective nominal power days, as shown in Figure 1. After submitting these data, users are shown either the amount of time required to reach the desired damage, or the amount of damage induced for a specified irradiation length at various irradiation positions, as shown in Figure 2. Users may then initiate the activation calculation by selecting a specific position to display for the activity for that material irradiation (see Figure 3).



The screenshot displays the NSUF Infrastructure website's 'Radioactivity and Damage Calculator'. The top navigation bar includes the NSUF logo and the user name 'Micah Gale'. The sidebar on the left lists various navigation options, with 'Calculator' currently selected. The main content area features a title 'Radioactivity and Damage Calculator' and three input fields: 'Calculation Type' (set to DPA), 'Desired DPA' (set to 1.5), and 'Material Composition' (set to Fe-17Cr-12Ni). A 'Calculate' button is positioned at the bottom right of the input fields.

Figure 1. The user input requesting the material to be irradiated and the desired amount of irradiation.

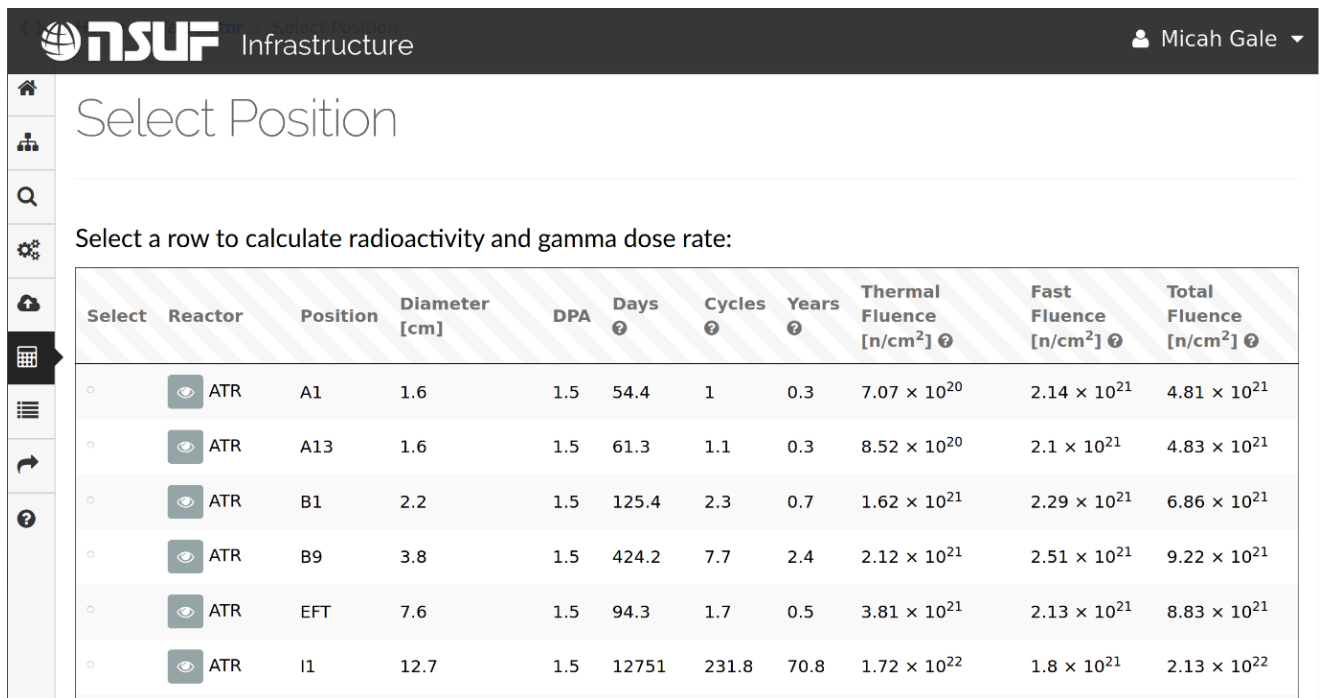


Figure 2. Example Output Showing Reactor Positions and Estimated Damage.

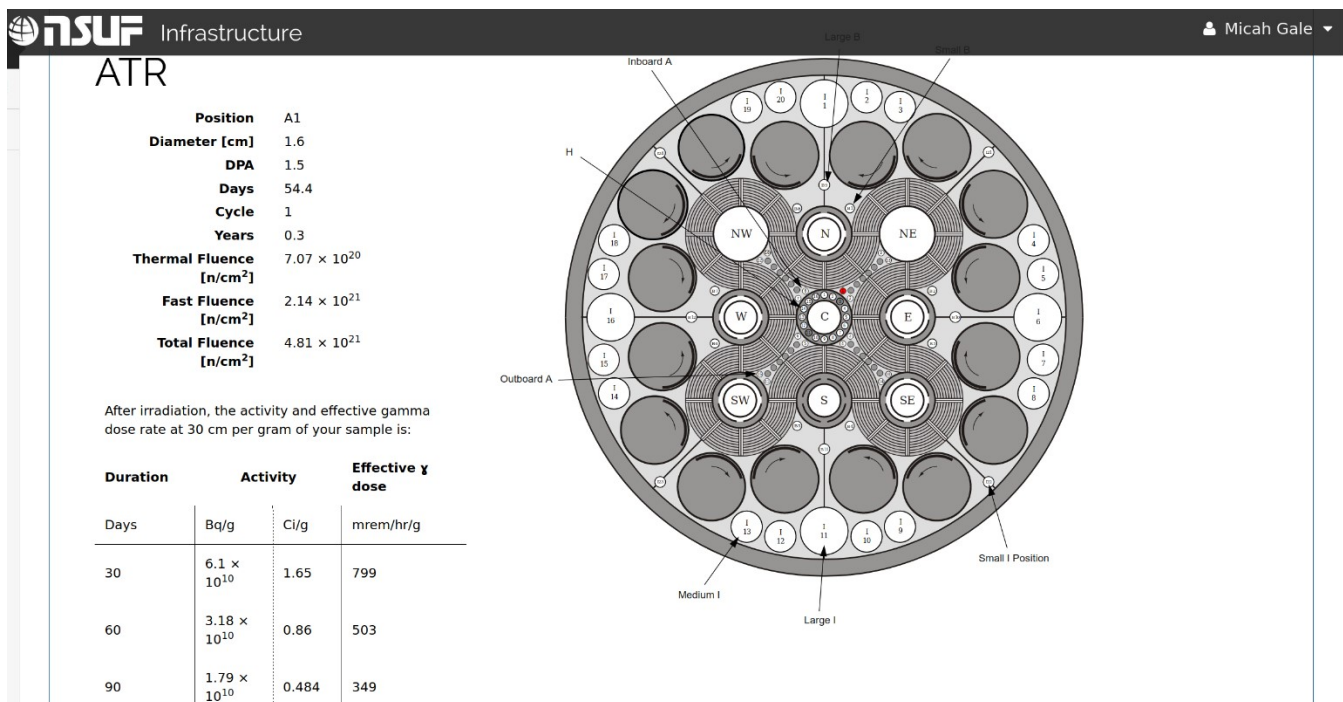


Figure 3. The specific activity of a material irradiated in a reactor position, based on user input.

The internal calculation process is shown in Figure 4. The user input is parsed and used to calculate radiation damage for various reactor positions. The user then selects a reactor position, sending data to the server regarding the position selected, the material, and the desired irradiation length. The calculator then activates the material via the method shown in Section 2.2. This solution of isotopic concentration is then

decayed through the same method. The isotopics are then used to find the total specific activity and gamma dose rate and present them to the user.

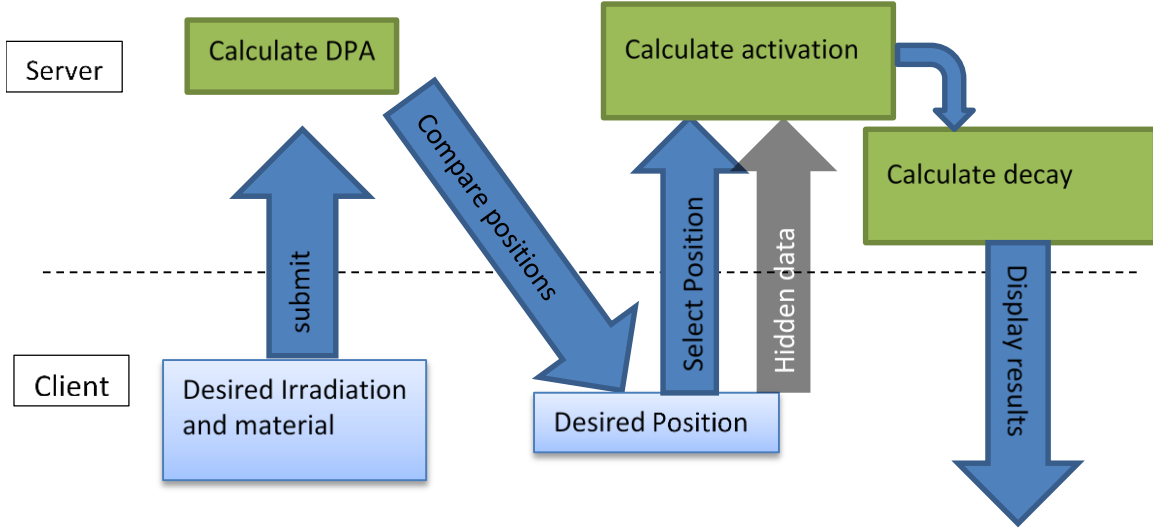


Figure 4. Block diagram of how the RAD calculator works and the interactions between client and server.

2. BACKGROUND

2.1 Theoretical Basis and Analytical Solution

The concentration of nuclide i in a neutron flux (ϕ) is governed by the ordinary differential equation (ODE):

$$\frac{\partial N_i}{\partial t} = \sum_j [\lambda_{j \rightarrow i} N_j(t) + \int_0^\infty \sigma_{j \rightarrow i}(E) N_j(t) \phi(E) dE] - \sum_j [\lambda_{i \rightarrow j} N_i(t) + \int_0^\infty \sigma_{i \rightarrow j}(E) N_i(t) \phi(E) dE] \quad (1)$$

Where:

- N_i is the isotopic concentration for isotope i $\left[\frac{\text{atoms}}{g}\right]$
- $\lambda_{x \rightarrow y}$ is the radioactive decay constant for isotope x decaying to isotope y $[s^{-1}]$
- $\sigma_{x \rightarrow y}$ is the microscopic cross section of isotope x for the (n,X) reaction to produce isotope y [barns, b]
- ϕ is the scalar neutron flux $\left[\frac{n}{cm^2 s}\right]$
- E is the neutron energy [eV] [2].

It should be noted that the flux is temporally- and spatially- independent, and therefore implicitly includes the following assumptions:

1. The sample of interest is sufficiently small with respect to the mean free path of the neutron, such that flux gradients within the sample are negligible.
2. The scalar flux is constant over time, and there are no outages or power variations.
3. Although not required, it is commonly assumed the sample is, in effect, infinitely dilute, such that it in no way perturbs the flux and has no self-shielding effects.

From this ODE, it becomes apparent there exists a system of coupled ODEs that cannot be solved in a de-coupled way, due to the coupling of nuclide concentrations in the same activation and decay chain. This problem is well-suited for linear algebra: N_i are combined into concentration vector \vec{N} . A transmutation matrix, F , which contains the specific reaction rates, can be constructed such that [3]:

$$\frac{\partial \vec{N}}{\partial t} = F\vec{N}(t) \quad (2)$$

If $\vec{N}(t = 0) \triangleq \vec{N}_0$, this ODE has a simple analytical solution:

$$\vec{N}(t) = e^{Ft} \vec{N}_0 \quad (3)$$

However, this solution must be used with caution, as each method for the numerical approximation of a matrix's exponential is only convergent for specific Eigen-spaces [3].

2.2 Implemented Solution Method

2.2.1 Nuclear Data Resources

The current implementation of the activation calculator solves this system of material-activation ODEs through the Chebyshev Rational Approximation Method (CRAM), which numerically approximates the matrix exponential, among other functions [4].

The reactor fluxes were generated via an MCNP [5] model of a nominal loading for each reactor. These fluxes are stored in a 252-group structure first established for use in the SCALE-6.2.3 code suite [2]. All cross sections were doppler-broadened to 600 K, then collapsed from point-wise cross sections into the aforementioned group structure using NJOY, a nuclear data processing code [6]. The nuclear data came from ENDF/B-VIII.0 [7], JEFF-3.2 [8], or TENDL-2017 [9]. The data were used in that order dependent on the availability of these data. During the group cross-section collapse a fission spectrum was assumed for fast neutrons, a $\frac{1}{E}$ flux was assumed for epithermal neutrons, and a 600 K (327°C, 628°F) Maxwellian distribution was assumed for thermal neutrons.

Prior to solving, the material isotopics are generated according to the weight fractions of the material composition supplied by the user, combined with the naturally occurring isotopics for each element [10]. These are stored as concentrations in atoms per gram of material. The decay chains are recursively built with a maximum recursion depth of 25 reactions.

The total number of days spent in the reactor is equal to the days of irradiation plus the inter-cycle outages. The irradiation length is a measure of the effective nominal power days. Nominal power is used instead of full power, since the Advanced Test Reactor (ATR) rarely runs at full power. Nominal power for the ATR is assumed to be 22 MW per lobe [11].

2.2.2 Building the Transmutation Matrices

Activation and decay reactions are both required for a proper material activation solution, but only decay reactions are needed for the decay cooldown periods. As a result, two transmutation matrices are created: one filled solely with activation reactions, the other filled solely with decay reactions. For the activation step, the activation and decay matrices are combined into a single transmutation matrix. These matrices are $N \times N$ matrices, where N is the number of isotopes. Since not every isotope has a reaction that can produce every other isotope, the matrix is relatively sparse. However, the matrices are stored as dense matrices because the chosen matrix solver can only work on dense matrices. Each cell in the matrix is filled according to:

$$f_{i,j} = \begin{cases} l_{i,j}\lambda_j + \sigma_{j \rightarrow i}\Phi, & i \neq j \\ -\lambda_i - \sigma_i\Phi, & i = j \end{cases} \quad (4)$$

Where:

- l_i is the decay branching ratio of isotope j decaying to isotope i
- λ_j is the decay constant for isotope j [s^{-1}]
- $\sigma_{j \rightarrow i}$ is the cross section for the reaction producing isotope i from isotope j [b]
- σ_i is the total absorption cross section for isotope i
- Φ is the scalar flux [$\frac{n}{cm^2s}$] [2].

The list of isotopes of interest is compiled beforehand by recursively building the activation/decay chain from the naturally occurring isotopes in the sample. The recursion is limited to a depth of 25 reactions. The matrix solver is more efficient if the transmutation matrix is an upper triangular matrix. The isotopes are sorted to form the transmutation matrices as close to this as is there is no way to form a truly upper triangular matrix with these data. This is done by sorting them in ascending order according to their ZAID number; namely, Z (atomic number)*10,000 + A (atomic mass)*10 + I (isomeric state). This gets the matrix as close to an upper triangular form as possible. This system makes it so that the (n, γ) activations, which are common, are represented just below the matrix diagonal.

2.2.3 Solving the Matrix Exponential with a Rational Approximation.

There are many ways to solve the matrix exponential. For those eigenspaces the transmutation matrices would occupy, CRAM is an extremely accurate and fast approximation. It was shown that the error of the solution was relatively unimpacted by the material composition and irradiation time step used [3].

The goal of CRAM is to find a rational function of polynomials that approximates the exponential function. Since this is a function based on polynomials, all that needs to be found are the coefficients for these polynomials. Once found, they can be applied to any other similar problem. The function to be found is of the form:

$$r_{k,k}(z) = \frac{p_k(z)}{q_k(z)} \quad (5)$$

Where:

- $r_{k,k}$ is the rational function that will approximate the matrix exponential
- p_k and q_k are both polynomials of order k
- z is an arbitrary input.

The partial fraction decomposition of this arbitrary rational function can then be simplified as:

$$r_{k,k}(z) = \alpha_0 + \sum_{j=1}^k \frac{\alpha_j}{z - \theta_j} \quad (6)$$

Where:

- α_0 is the limit of $r_{k,k}$ as z approaches infinity

- α_j is the residue at corresponding pole θ_j .

Since, the poles of a rational function with real-valued coefficients form conjugate pairs, only half of the values need to be computed:

$$r_{(k,k)}(z) = \alpha_0 + 2\text{Re} \left(\sum_{j=1}^{k/2} \frac{\alpha_j}{z - \theta_j} \right) \quad (7)$$

Substituting Equation 3 into Equation 7 then yields:

$$n(t) = \alpha_0 n_0 + 2\text{Re} \left(\sum_{j=1}^{\frac{k}{2}} \alpha_j (At - \theta_j I)^{-1} n_0 \right) \quad (8)$$

The coefficients must now be calculated. Fortunately, Dr. Maria Pusa completed this for a rational function of orders 14 and 16 [4]. A rational function of order 16 is used in the calculator.

The coefficients tabulated by Pusa are complex numbers. In addition, it is faster to solve a matrix system of equations than to invert a matrix. So, a linear algebra library capable of solving complex matrix equations was needed. This web application was written in C#, so Math.net Numerics [12] was used to handle the linear algebra, with complex numbers represented by the Complex Struct in System.Numerics. The Complex Struct stores both the imaginary and real parts of the number as double-precision floating-points [13].

The activation and decay transmutation matrices are added together for the irradiation. Then, the isotopic quantities are calculated for the whole irradiation length in a single step. Next, the decays are calculated solely through the decay matrix. The decay matrix is used four times to calculate the isotopic concentrations for each decay length displayed to users.

2.3 Acceptance Criterion

The metric of success used in this report is the percentage of test cases run where the results of that run were within $\pm 50\%$ of the output for the same input conditions run in the ORIGEN module of SCALE-6.2.3. In the NSUF Combined Material Experiment Toolbox (CoMET) Project Implementation Plan, INL/EXT-19-53000, the acceptance criterion is defined as follows:

The calculator shall be within $\pm 50\%$ of the correct answer, with conservative biases preferred. In this case, overpredicting the gamma dose rate and activity would be conservative. If an element does not fall within these bounds, the user must be warned of the inaccuracy.

This step ensures that the users are cautioned in the cases where the calculator compares poorly to ORIGEN. The 50% tolerance is based on the mission of the RAD Calculator: to be a scoping tool to aid researchers in planning an irradiation experiment and the associated post-irradiation examination. It is not intended to replace the formal analyses performed by the technical staff at the relevant NSUF partner institutions. Those analyses help ensure the safety of the experiment. The RAD Calculator is only a tool to aid in planning.

2.4 Reactor Power Levels Used

Assumptions needed to be made about the nominal power levels for the reactors included in the calculator, and their operating cycles. These data are provided in Table 1.

Table 1 Power levels and operating cycles used by the calculator for the included reactors.

Reactor	Power Level [MW _{th}]	Cycle Length [days]	Effective Full Power Days per year
ATR	110 (22/lobe)	55	180
HFIR	85	27	189
MITR	6	63	252
PULSTAR	1	87*	87*

*PULSTAR Does not operate 24 hours day. This is calculated assuming they operate every workday including holidays.

2.5 Potential Failure Modes

Four main failure modes were found during the investigation of the set of out-of-tolerance results. These can occur independently or in multi-mode failures. The modes are (1) overproducing the daughter products, (2) underproducing the daughter products, (3) missing a long-lived daughter product, and (4) missing a short-lived daughter product.

2.5.1 Time-Invariant Failure Modes

Many of the elements' activities over- or undershoot the actual activity. In an independent failure without missing isotopes, this is characterized by an error rate that does not vary in accordance with cooldown time. This is because the initial quantity to decay is wrong, but the decaying proceeds properly, thereby maintaining the error as a constant multiple between the two decay curves. This is likely caused by missing cross sections. If the nuclear data for an important reaction are wrong or missing, the incorrect reaction rate shifts the solution. If a competing reaction for an intermediary product is missing, the equilibrium concentration for that product will be too high, leading to errors in the final solution.

2.5.2 Time-Variant Failure Modes

A missing radioisotope in the activation/decay chain is characterized by a time-variant error in the results. This time-variant error during cooldown is caused by the isotopes decaying at different rates and causing the magnitude of the error to grow or shrink.

- If the magnitude of error increases over time, this is caused by a missing long-lived isotope as the shorter-lived isotopes decay, leaving very little radioactive material with respect to the benchmark solution.
- If the magnitude of error decreases over time, this is caused by a missing short-lived isotope. The short-lived isotope decays and has a lesser impact on the solution over time.

3. ANALYSIS

3.1 Benchmark Validation Against ORIGEN

A benchmark case was generated using the ORIGEN module in SCALE 6.2.3 [14]. This benchmark calculated the activation and subsequent decay for 81 elements using each element's natural isotopes. It reported the specific gamma dose rate [mrem/hr/g] at 30 cm from the sample, for 30, 60, 90, and 180 days after irradiation. All data were collected via a custom python [15] script that automatically queried the RAD Calculator website and scraped the necessary data. The script also automatically ran SCALE 6.2.3 and parsed the output. NSUF's access to the INL high-performance computing resources was utilized to increase the speed of this large set of calculations. The same fluxes used by the calculator were used to produce the reaction-rate libraries for ORIGEN using the COUPLE module in SCALE.

The python script used gamma-factor data from the calculator to calculate the gamma dose rate at 30 cm. The calculator does not track metastable isomers; rather, it assumes all the atoms of an isotope are in one isomeric state. This state is chosen based on which one (ground or metastable) most contributes to the specific gamma dose rate. ORIGEN tracks specific isomers, and only those with a gamma factor in the calculator were used. This may lead to the ORIGEN benchmark slightly overpredicting the specific gamma dose rate, but this is negligible compared to the desired 50% accuracy threshold set for the calculator.

Data were collected for all 81 elements and all positions included in the calculator for the following irradiation times: 0.1, 1, 7.5, 15, 30, 60, 120, 180, 240, 360, 480, 720, and 960 days. These time steps were chosen in order to provide ample coverage for most of the logarithmic decades considered by the calculator. The elements excluded were synthetic elements (e.g., technetium), or elements with an atomic number greater than that of bismuth (83). Technically, some elements with atomic numbers higher than that of bismuth are naturally occurring, but they exist in such vanishingly small quantities that a natural source cannot be used, and they would have to be synthesized. These elements are excluded because the exact isotopes need to be known and would have to be user-supplied. Thorium and uranium are excluded for the same reason — being so commonly enriched as to make it very ambiguous what the user intended for them. Figure 5 – 8 show maps for the reactor cores included in the calculator.

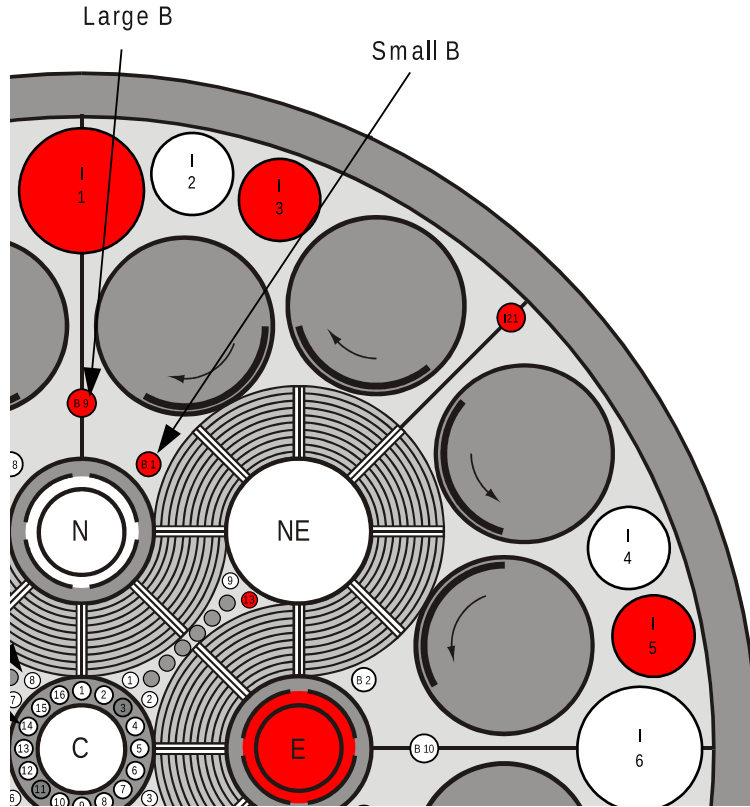


Figure 5. Core map for the ATR showing positions included in the calculator. The positions in red are those included in the calculator. The core is quadrant symmetric, so representative positions were used.

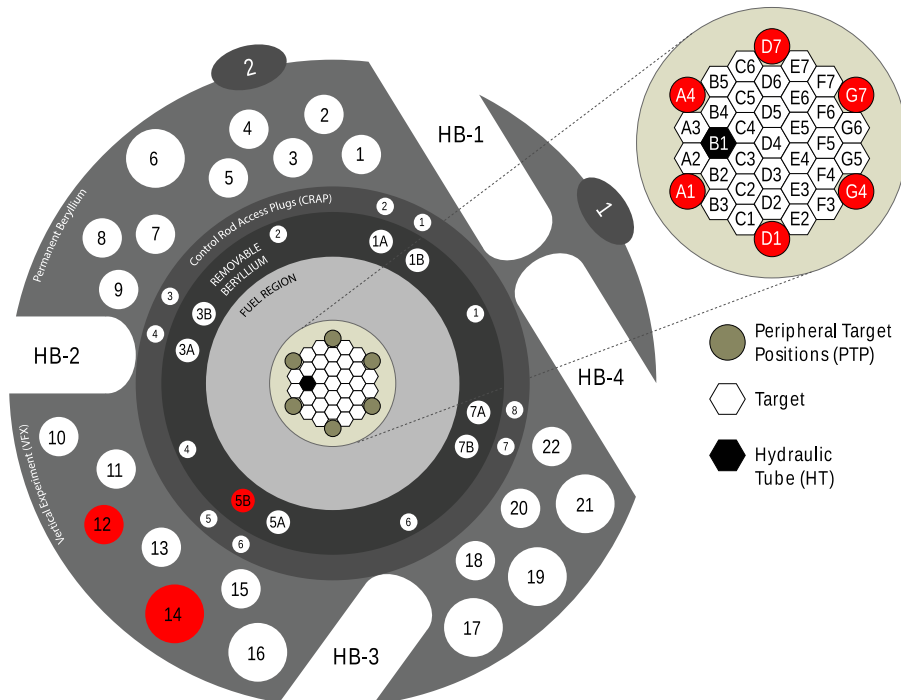


Figure 6. Core map for the High Flux Isotope Reactor (HFIR). The positions in red are included in the calculator and were chosen as representative positions.

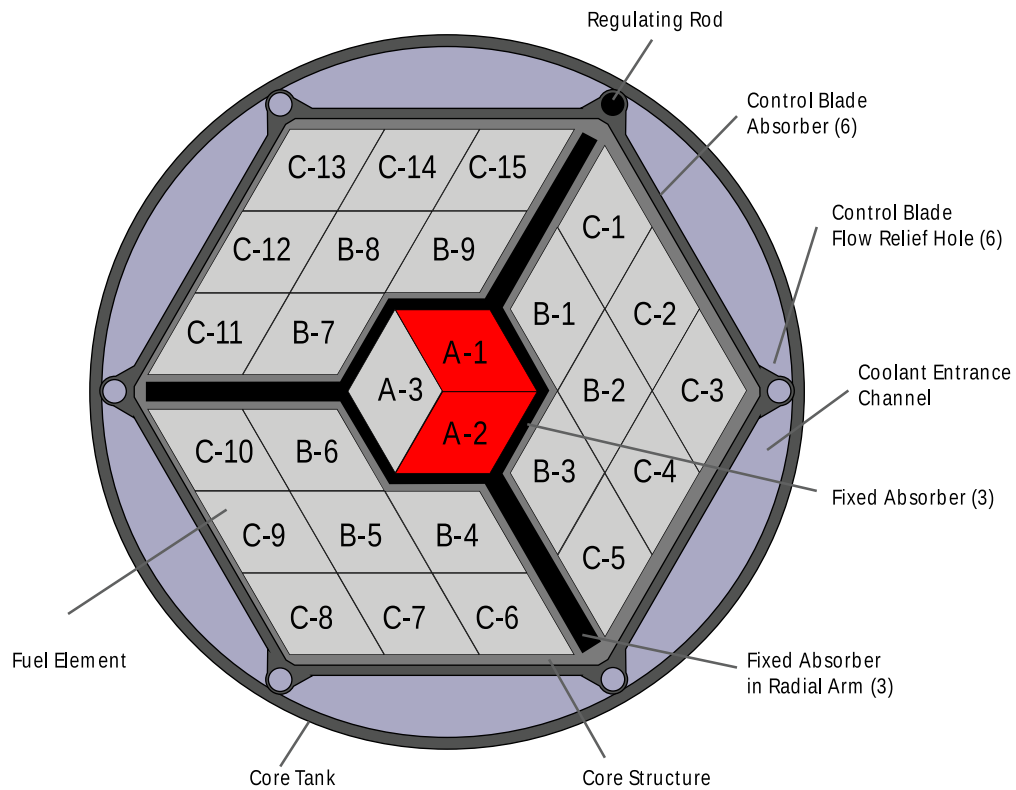


Figure 7. Core map for the Massachusetts Institute of Technology Reactor-II (MITR-II). The positions in red are those included in the calculator.

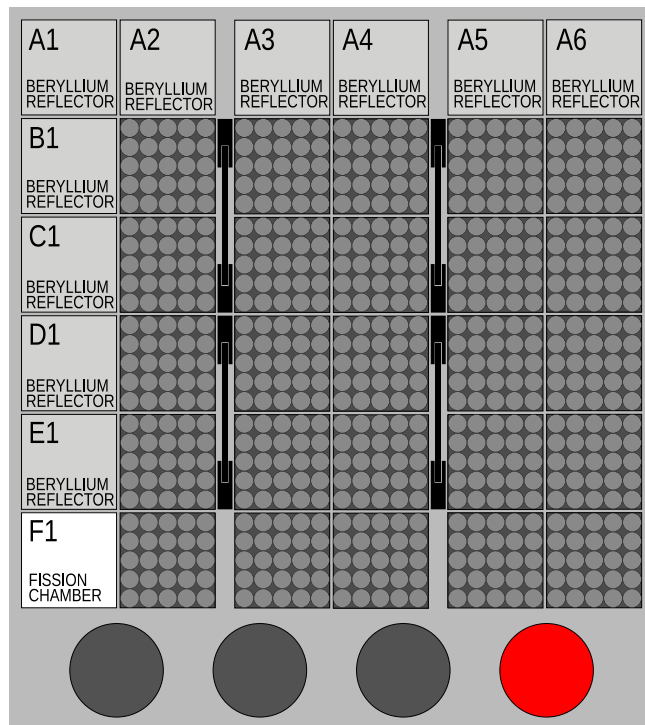


Figure 8. Core map for North Carolina State University's PULSTAR Reactor. The position in red is included in the calculator

Another python script was used to compare all conditions of irradiation length, reactor position, the element irradiated, and the cooldown time between the RAD calculator and the ORIGEN benchmark. These comparisons were done by calculating the percent difference from ORIGEN, such that a positive value means the RAD calculator overpredicted the dose rate, and a negative value means it underpredicted the dose rate.

Initial analysis was completed by determining the amount of materials which were within tolerance. This was done by having a moving tolerance threshold and finding all test cases that did not meet this accuracy threshold. Various acceptance thresholds were set; these were 0%, 10%, ..., 90%, and 100%. For each of these thresholds, it was found how many of the tests were not within that threshold (e.g. 10%) of the answer generated by ORIGEN. In many cases, unnecessary errors were due to different minimum cutoff thresholds. To prevent this from causing misleading errors, a high-pass filter of 0.1 mrem/hr/g was used for the ORIGEN benchmark. This was chosen since 1 kg of samples would exceed the typical facility limit of 100 mrem/hr at 30 cm.

Initially, this analysis was performed by viewing irradiation length as the independent variable, shown in Figure 9. In this figure, each color band represents a looser acceptance criterion when going from green to red to magenta. The first dark green band represents an acceptance threshold of 0%. All tests have an error greater than or equal to 0% so this forms a line at 100%. The next band down represents an acceptance criterion of 10%, and so on and so forth. The red band illustrates an acceptance criterion of $\pm 50\%$, which is the criterion used for the RAD calculator. One sees a logarithmic relationship between irradiation length and the error. This suggests there are no divergent solutions or other errors caused by the solver itself. The error is likely caused by missing nuclear reaction data. To test this, there should be a strong correlation between error and elements irradiated.

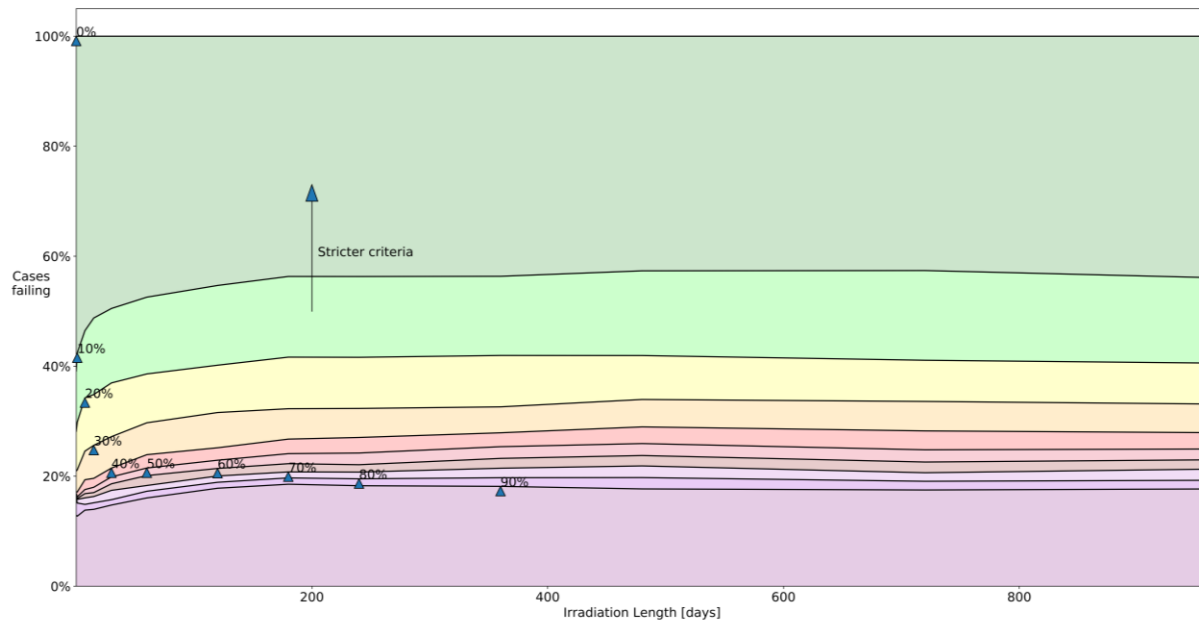


Figure 9. Accuracy of the RAD calculator when compared to ORIGEN based on simulated irradiation length. Each color band represents a range of absolute percent differences between the RAD calculator and ORIGEN. The y-axis is the proportion of cases falling within these various tolerance bands. A high-pass filter of 0.1 mrem/hr/g for the ORIGEN test case was applied to remove the effects of different cutoff thresholds.

In Figure 10, this hypothesis was tested by comparing these error rates for each element tested. A similar plotting system was used in this figure as was used in Figure 9. For example, titanium has a single dark green bar in the range 0% – 100%. This means that for all test cases titanium had an error of

less than $\pm 10\%$. On the other end, vanadium has a dark magenta bar that spans the same range. This means that for all test cases vanadium has an error greater than $\pm 90\%$. One clearly sees that the primary source of error is erroneous/missing nuclear data, as the error is highly dependent on the starting element. In general, the dose rate from an irradiated element is either highly accurate or highly erroneous. This clearly merits further review in order to find and add these missing reactions.

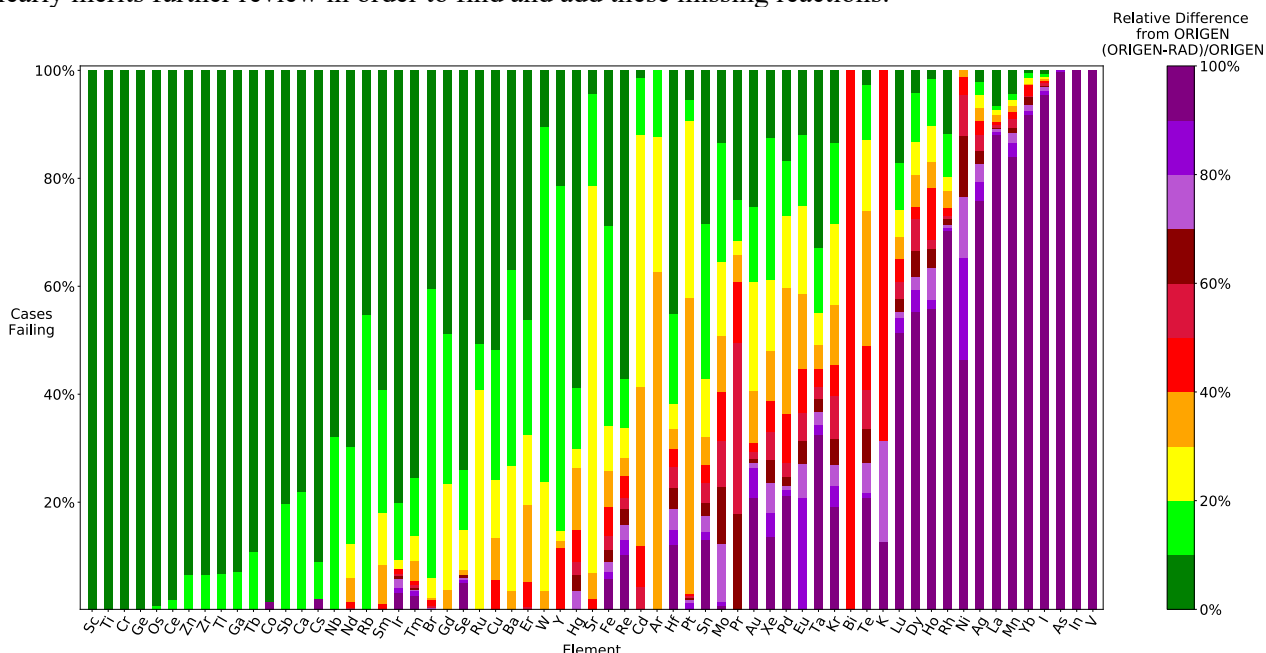


Figure 10 The accuracy of the RAD calculator compared to ORIGEN for specific gamma dose rate with respect to the simulated element irradiated. Each color band represents a range absolute percent differences between the RAD calculator and ORIGEN. The y-axis is the number of cases falling within these various tolerance bands. A high pass filter of 0.1 mrem/hr/g for the ORIGEN test case was applied to remove the effects of different cutoff thresholds.

To be thorough, the contributions of individual reactor positions to the error rates need to be investigated. These results are shown in Figure 11. There is clearly some correlation between reactor positions and error, but there are no obvious outliers. Likely, these changes in error are due to the different flux spectrums for each reactor position, which cause different positions to over- or under-emphasize the missing nuclear data from before.

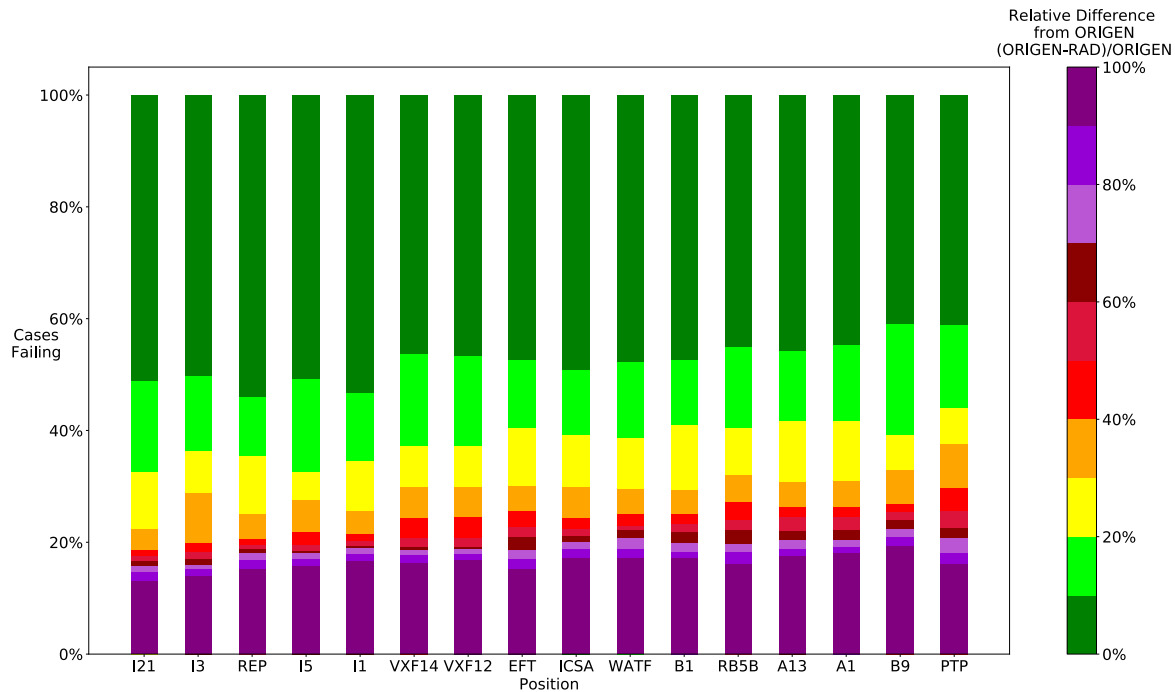


Figure 11. Accuracy of the RAD calculator compared to ORIGEN for specific gamma dose rate with respect to the reactor position used. Each color band represents a range of absolute percent differences between the RAD calculator and ORIGEN. The y-axis is the number of cases falling within these various tolerance bands. A high-pass filter of 0.1 mrem/hr/g for the ORIGEN test case was applied to remove the effects of different cutoff thresholds.

3.1.1 Benchmark Validation for Elements of Interest Only

Clearly, certain elements need further investigation. To prioritize efforts for such investigation, the list of elements was narrowed down to those currently in use in the Nuclear Fuels and Materials Library (NFML). The NFML is populated from previous NSUF experiments, legacy EBR-II (experimental breeder reactor-II) and FFTF (fast flux test facility) materials, and other donated nuclear materials. In this way, priority can be given to those materials most likely to be involved in future NSUF experiments. These elements are:

- | | | | |
|------|------|------|------|
| • Fe | • Si | • W | • Mn |
| • Al | • Ti | • Mo | • V |
| • C | • Nd | • Ni | • Y |
| • Co | • Nb | • Cu | • Zr |
| • P | • Ta | • Cr | |

The updated material graph featuring only the elements of interest listed above is shown in Figure 12. It is clear that V, Mn, and Ni are all outliers, with Fe, Mo, and Ta faring worse than other elements. The elements V, Mn, Mo, Ta are often used in structural materials as additives in small quantities, so their impact to the overall activity of the sample will not be large, maintaining an accurate enough answer for scoping out an experiment. Iron and nickel are more important though, due to their prevalence and use in steels.

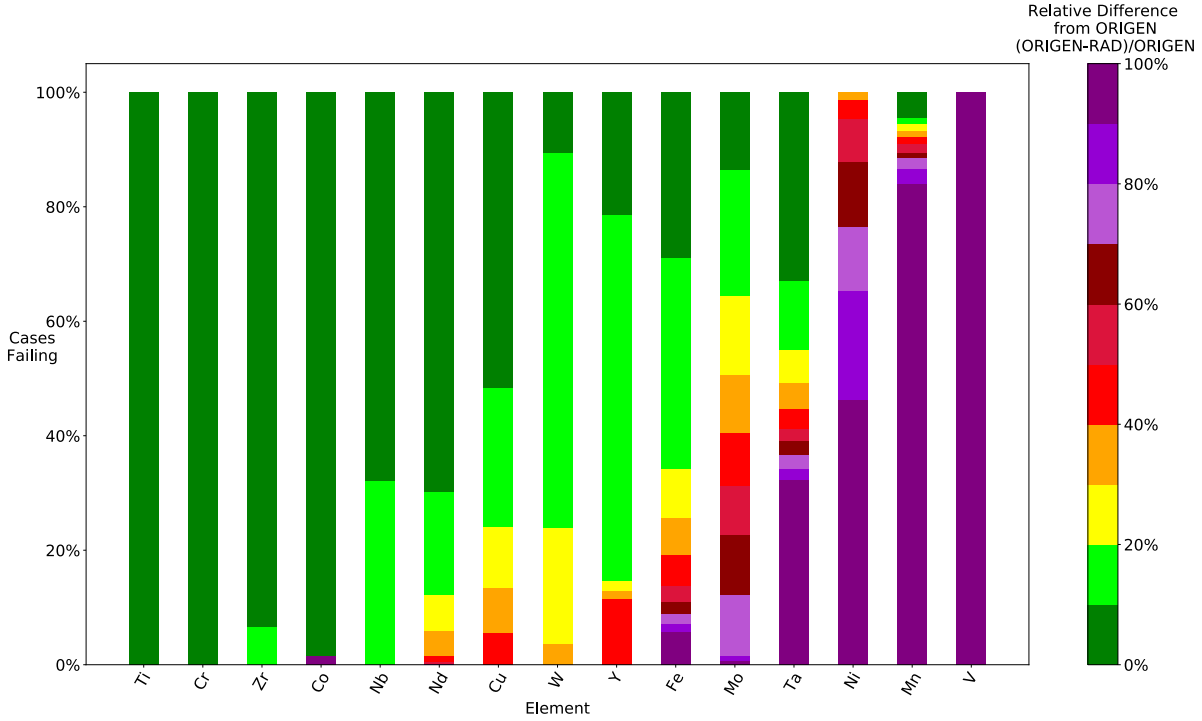


Figure 12. Accuracy of the RAD calculator, as compared to ORIGEN, for specific gamma dose rate with respect to the simulated element irradiated. Only materials in the NFML are included. Each color band represents a range of absolute percent differences between the RAD calculator and ORIGEN. The y-axis is the number of cases falling within these various tolerance bands. A high-pass filter of 0.1 mrem/hr/g for the ORIGEN test case was applied to remove the effects of different cutoff thresholds.

With this refined list of materials, the behavior of the rate of errors over time does not significantly change; the overall error is simply reduced as shown in Figure 13. This shows there is no extreme or unexpected behavior for these specific materials. Neither do we see anything extraordinary when looking at the errors in accordance with the positions as shown in Figure 14. The correlation between position and rate of error is stronger for these elements and may need to be evaluated on a case-by-case basis.

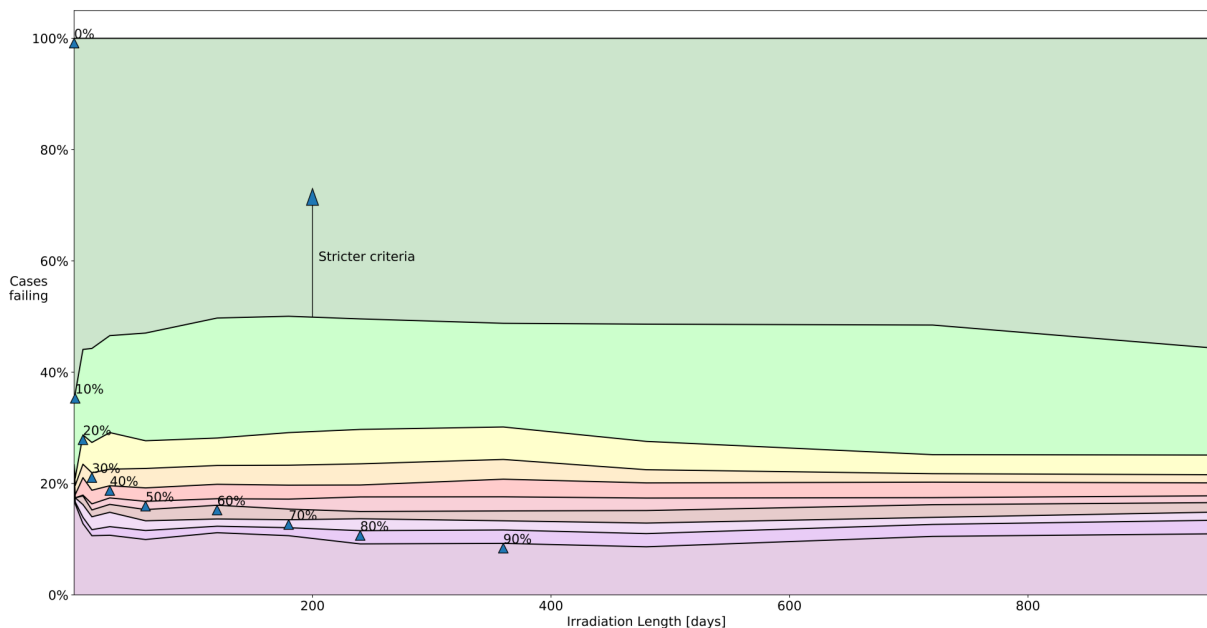


Figure 13. Accuracy of the RAD calculator, as compared to ORIGEN, for specific gamma dose rate with respect to the simulated irradiation length. Only materials in the NFML are included. Each color band represents a range of absolute percent differences between the RAD calculator and ORIGEN. The y-axis is the number of cases falling within these various tolerance bands. A high-pass filter of 0.1 mrem/hr/g for the ORIGEN test case was applied to remove the effects of different cutoff thresholds.

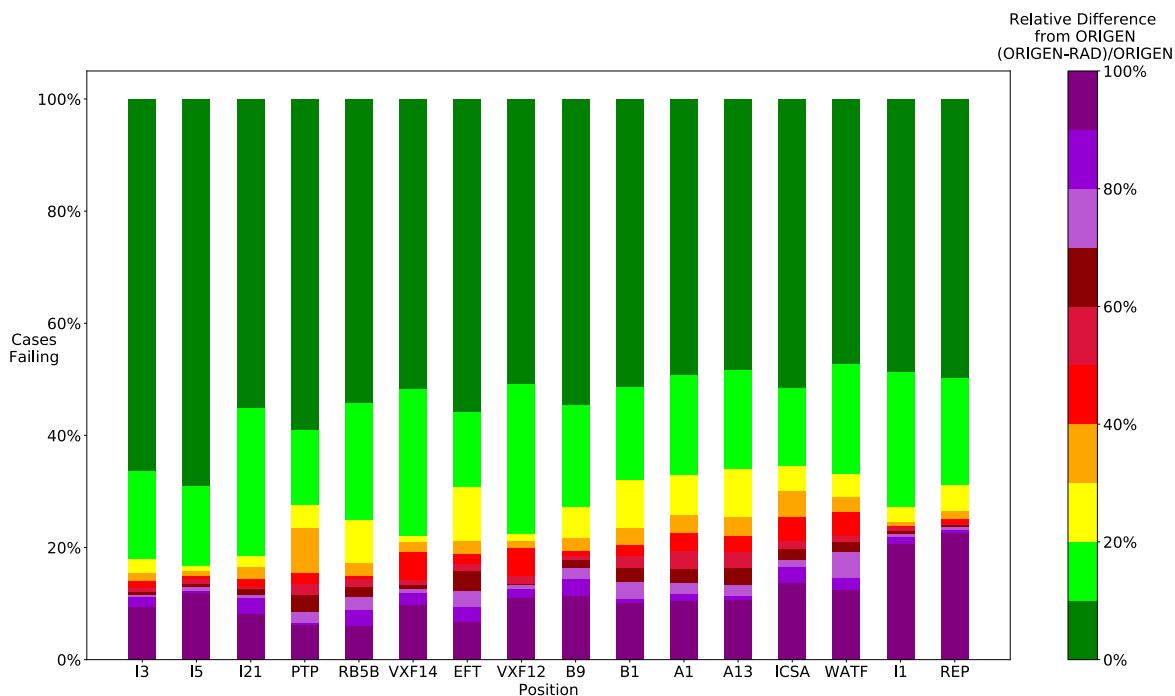


Figure 14. Accuracy of the RAD calculator, as compared to ORIGEN, for specific gamma dose rate with respect to the reactor position used. Only materials in the NFML are included. Each color band represents a range of absolute percent differences between the RAD calculator and ORIGEN. The y-axis is the number of cases falling within these various tolerance bands. A high-pass filter of 0.1 mrem/hr/g for the ORIGEN test case was applied to remove the effects of different cutoff thresholds.

3.1.2 Out-of-Tolerance Elements

A list was generated of elements that did not fall within the acceptance criterion for the calculator (see Table 2). These elements each had at least one test case that differed from ORIGEN by more than the acceptance criterion of $\pm 50\%$, and for which the ORIGEN benchmark produces at least 0.1 mrem/hr/g of specific gamma dose rate at 30 cm. This filter was chosen since 1kg of samples would exceed the 100 mrem/hr gamma dose rate at 30 cm threshold set by many radiological facilities. The average error was calculated by simply averaging all that element's differences in all test cases exceeding the high-pass filter. Note that some elements have an average error of 0. This is because the element does create large errors in some cases, but the errors both over- and under-predict the gamma dose rate, cancelling each other out.

Table 2. Elements that, at least in one test case, fall outside the acceptable tolerance range. Elements of interest to the NFML are those currently contained in samples in the NFML.

Element	Included in the NFML	Average Error
V	Yes	-100%
Mn	Yes	-90%
Fe	Yes	30%
Ni	Yes	-80%
Cu	Yes	10%
Y	Yes	0%
Mo	Yes	-30%
Nd	Yes	0%
Ta	Yes	1,800%
K	No	60%
Co	No	50%
As	No	-100%
Se	No	20%
Br	No	-10%
Kr	No	20%
Sr	No	20%
Rh	No	2,000%
Pd	No	200%
Ag	No	750%
Cd	No	-30%
In	No	-100%

Element	Included in the NFML	Average Error
Sn	No	40%
Te	No	-50%
I	No	-100%
Xe	No	40%
Cs	No	40%
La	No	4,900%
Pr	No	-40%
Sm	No	0%
Eu	No	-30%
Dy	No	160%
Ho	No	200%
Tm	No	10%
Yb	No	8,000%
Lu	No	60%
Hf	No	50%
Re	No	-20%
Ir	No	0%
Pt	No	-30%
Au	No	-30%
Hg	No	-20%
Bi	No	40%

3.1.2.1 In-Depth Analysis of Iron

Further analysis is needed for iron, since it is such a key element in most NSUF experiments. In Figure 15, error rates for iron in various reactor positions are compared to the fast flux ratios of that position. The near step change in error for higher fast-to-total flux ratios indicates a strong correlation. We define fast flux as having $E > 100$ keV.

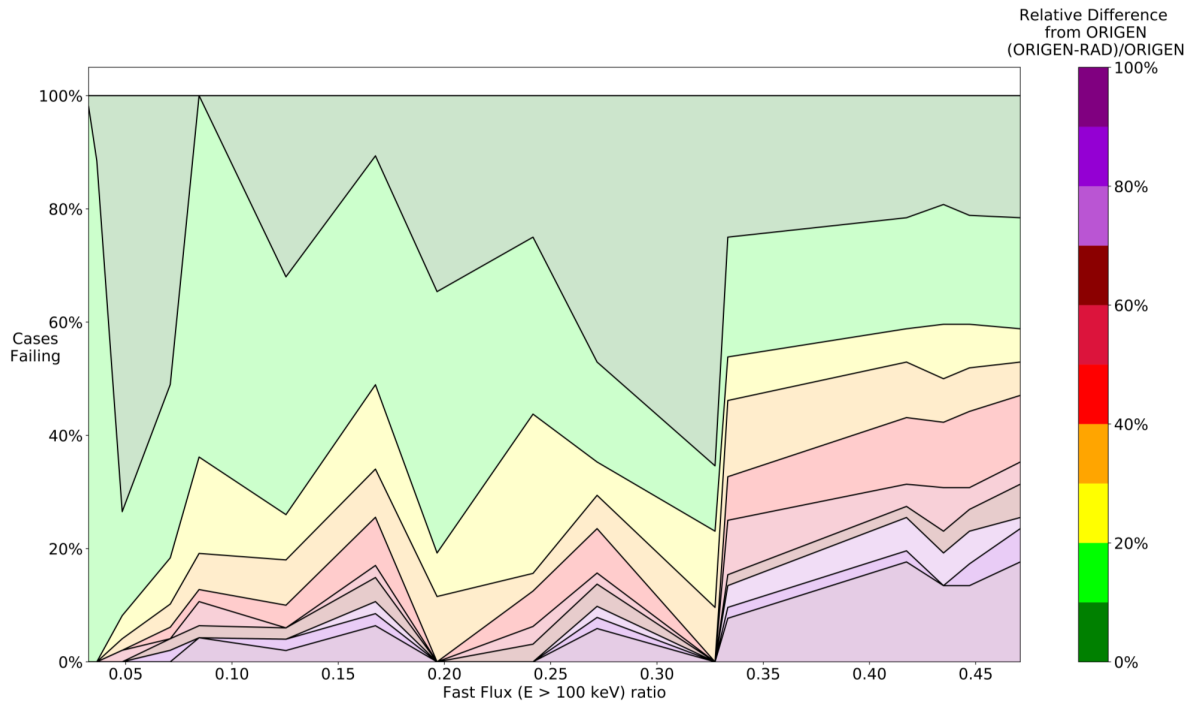


Figure 15. Accuracy of the RAD calculator, as compared to ORIGEN, for specific gamma dose rate for iron with respect to the fast-to-total-flux ratio for each reactor position. For this case, the fast flux cutoff is 100 keV. Each color band represents a range of absolute percent differences between the RAD calculator and ORIGEN. The y-axis is the number of cases falling within these various tolerance bands. A high-pass filter of 0.1 mrem/hr/g for the ORIGEN test case was applied to remove the effects of different cutoff thresholds.

Next to be investigated was the time evolution of the error for iron in the MITR-ICSA position (see Figure 16). This position was chosen as it was a position which was producing some of the highest error rates for iron. Each line represents the trend of error during a cooldown period for various irradiation lengths. Two important notes: first, the RAD calculator overpredicts the gamma dose rate, making this a conservative error; and secondly, the error increases over time, suggesting an incorrect long-lived isotope. With the possible missing threshold reaction, there is likely a missing removal reaction—namely, a reaction that would remove a strong, long-lived gamma-emitter. This missing reaction leads to overpredicting the concentration of the emitter.

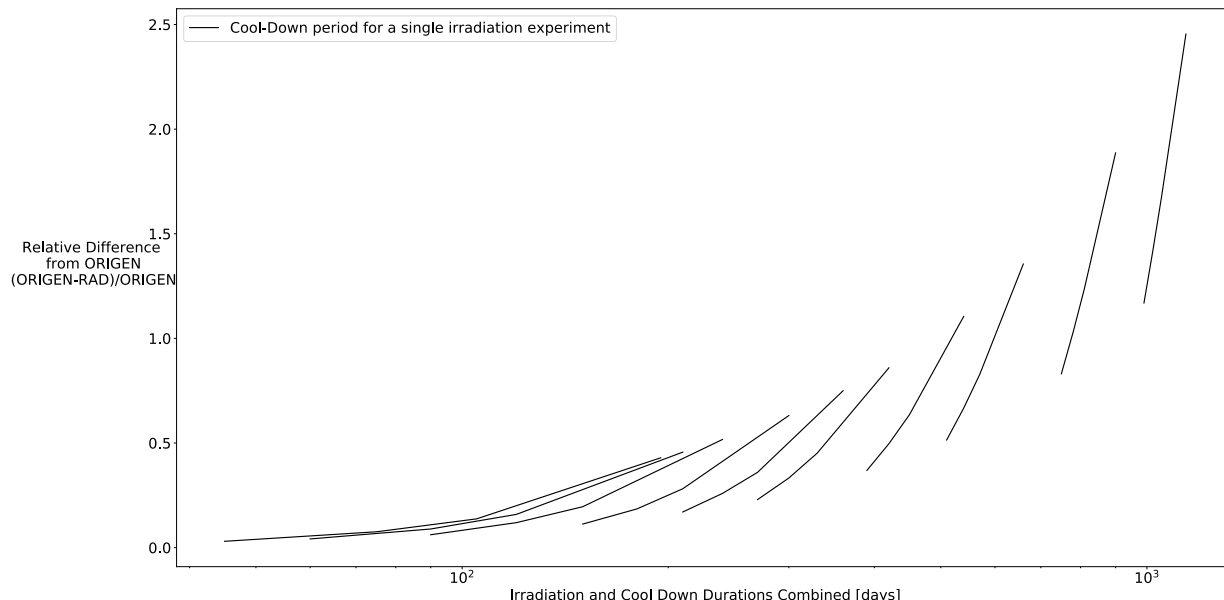


Figure 16. The relative difference between the RAD calculator and ORIGEN with respect to irradiation and cooldown time for iron in the MITR-ICSA position. The difference is calculated as $(\text{ORIGEN}-\text{RAD})/\text{ORIGEN}$. The irradiation duration and cool-down duration are combined on the x-axis. Each line represents a single irradiation and the associated cooldown period.

3.1.2.2 In-Depth Analysis of Nickel

Further analysis was performed on nickel, the other high-priority material needing examination. The time evolution was also analyzed for nickel in the MITR ICSA position (see Figure 17). This position was chosen since it produced similarly high amounts of error for nickel as well. For all irradiations, the error tended to underpredict the specific gamma dose rate during cooldown time, indicating the RAD calculator is missing the production of a key long-lived isotope. Also, the overall error decreases as irradiation length increases, suggesting that the missing isotope becomes less dominant with long irradiations as an even longer-lived isotope builds up in concentration almost linearly and more greatly dominates the emission source the longer the sample is irradiated.

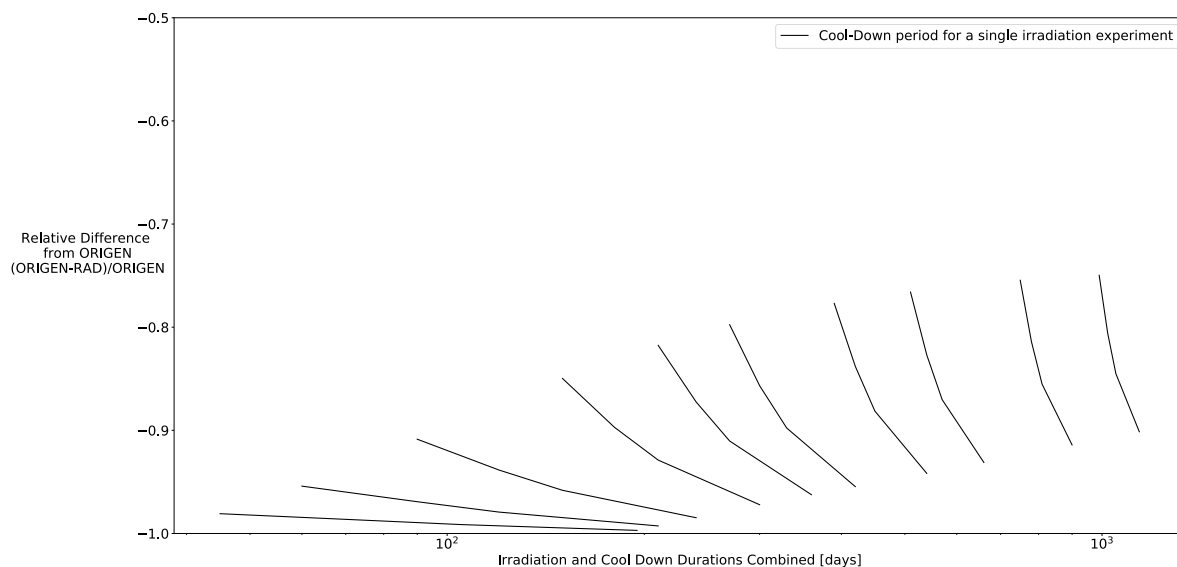


Figure 17. The relative difference between the RAD calculator and ORIGEN with respect to irradiation and cooldown time for nickel in the MITR-ICSA position. The difference is calculated as $(\text{ORIGEN}-\text{RAD})/\text{ORIGEN}$. The irradiation duration and cool-down duration are combined on the x-axis. Each line represents a single irradiation and the associated cooldown period.

3.1.3 Convergence of the ORIGEN Solution

There was concern over whether some of these errors were caused by the RAD calculator or by ORIGEN. To rule out ORIGEN, a bounding convergence case was performed using the “doubling method” whereby convergence-affecting parameters are doubled and variations between the two calculations are measured. In this case, the order of the CRAM [4] solver and the number of sub steps were varied to affect convergence. All benchmark calculations used a CRAM solver order of 16 with two sub steps.

Since the worst error for tungsten in ATR-B1 occurs at 720 days of irradiation, this is the irradiation case used. The two extremes were compared to create a bounding convergence case to justify the benchmark. Isotopics calculated for a solution of order 8 with one sub step were compared with the isotopics for a solution of order 16 with four sub steps. The CRAM solver in ORIGEN cannot work for orders higher than 16. The largest difference was 1.0544% for Pt-193, which has a concentration of 7.34×10^{-10} moles/g. The correct concentration for Pt-193 is small, especially when compared to the large acceptance criteria for the calculator. Since this is a more extreme convergence test than what is used to calculate the benchmark, this variation in the ORIGEN output is small enough to not affect the output of these analyses.

4. RECOMMENDATIONS

The NSUF RAD Calculator is a scoping tool for aiding researchers in determining approximate activity in order to better select appropriate post-irradiation-examination facilities. For elements of interest included in the NFML, the RAD calculator is within the stated tolerance for 83% of test cases. For the immediate term, this is adequate, and the RAD calculator needs to caution users when they are using elements with above-tolerance error; these elements are listed in Table 2. This report, along with the accompanying report for the radiation damage calculator, will be available at the RAD calculator website for reference.

4.1 Changes Needed Prior to Deployment

Prior to deployment, the calculator will be made to inform users when they request activations involving materials that significantly underpredict the gamma dose rate. These materials are listed in Table 2.

4.2 Medium-Term Changes (FY2020)

4.2.1 Improving Nuclear Data

Previous versions of the calculator used an Euler's method based solver, rather than a CRAM-based one. This led to accuracy issues due to divergence with large time-steps. This made it hard to determine if the errors were due to the solver, or the underlying nuclear data. With the CRAM-based solver implemented, all errors should now be investigated under the assumption that missing nuclear data are at fault. Top priority should be given first to nickel, then iron, followed by elements currently used in samples in the NFML, followed by all other elements.

4.3 Long-Term Changes (FY2021)

In the long-term, fundamental components of the RAD Calculator should be examined and analyzed to determine whether they are optimal. As stated in Section 2, many assumptions are built into the calculator methods. These assumptions inherently limit the regime of accurate estimates. This bounding box should be discovered, and the question of whether these bounds are acceptable should be examined.

4.4 Other Calculator Modifications and Features to Consider

These are some features, and other considerations to investigate once all the fundamental nuclear data issues are solved.

4.4.1 Calculator Assumptions

A key assumption in the calculator is that the materials have similar neutron transparency and dilution to iron, meaning they cause no flux perturbations dissimilar to that caused by the simulated iron targets. This may be valid for materials with cross sections similar to iron's, but it quickly breaks down with heavier elements such as europium. These large absorption cross sections cause larger flux depressions. Missing these flux depressions always causes the activity to be overpredicted, because the self-shielding effects are underrepresented. An analysis of these self-shielding effects should be considered; the simplest method to deal with self-shielding effect being the narrow/wide resonance approximations. (Intermediate resonance approximation requires a higher degree of sophistication.) Finally, the highest fidelity approach would be to run a method of characteristics, Monte Carlo, or other neutronic simulation. This could be done on the fly or ran once and cached. Ignoring self-shielding effects results in conservative estimates being produced.

The other assumption is that the reactor always runs at nominal power for the length of irradiation. This is valid for a single irradiation campaign, but for longer irradiations, decays during outages would

cause the calculator to over-predict the activity of the samples, which is conservative. The effects of these outages should be considered. One solution is to assume a typical outage schedule and explicitly decay the material accordingly. Using the CRAM solver, these outages could be quickly calculated.

4.4.2 Implementation of Fuel Calculations

Performing an accurate fuel depletion calculation is complicated and difficult. It is not impossible, but many core assumptions of the calculator are invalid for fissile and fertile materials. Though not an exhaustive list, here are some of the complications that need to be considered.

4.4.2.1 Figures of Merit

Currently for damage calculations, DPA is used as the figure of merit. This works well for structural materials but breaks down with fuels due to internal fission. The damage calculator would need to be updated to allow other figures of merit such as burnup and fission density.

4.4.2.2 Flux Perturbations

Having a fueled experiment creates a large flux perturbation and reactivity change. This reactivity insertion may require shifting of fuel, causing the incident flux to harden or soften. In addition, the fuel will become a fast neutron source and likely hold very strong resonance absorbers (e.g., U-238) that alter the flux shape. If the fuel samples are any larger than the smallest discs, the only way to handle this will be to run some form of neutronics analysis on the fuel. Even if the fuel is purely fertile and causes no fissions, it will cause enough self-shielding to break the infinitely dilute assumption, and case-specific fluxes and cross sections will be required for most fuel sample sizes. Analysis must be done to find the smallest sample size that can still cause flux perturbations.

4.4.2.3 Data Requirements

For handling fuel depletion, fission yields for most isotopes need to be added to the calculator. With fissions, many more decay chains are possible than through activation. These decay chains will need to be added and debugged.

5. REFERENCES

- [1] A. Mata Cruz and M. Gale, "Evaluation of the Reactor Activation and Damage (RAD) Calculator's Damage Component," Idaho National Laboratory, Idaho Falls, ID, Government Report INL/EXT-20-58365, Mar. 2020.
- [2] "SCALE Code System," Oak Ridge National Laboratory, Oak Ridge, TN, Government Manual ORNL/TM-2005/39 Version 6.2.3, Mar. 2018. [Online]. Available: https://www.ornl.gov/sites/default/files/SCALE_6.2.3.pdf.
- [3] M. Pusa, "Numerical methods for nuclear fuel burnup calculations: Maria Pusa.," Sc.D. Dissertation, Aalto University, Espoo, Finland, 2013.
- [4] M. Pusa, "Rational Approximations to the Matrix Exponential in Burnup Calculations," *Nuclear Science and Engineering*, vol. 169, no. 2, pp. 155–167, Oct. 2011, doi: 10.13182/NSE10-81.
- [5] C. J. Werner *et al.*, "MCNP Version 6.2 Release Notes," LA-UR-18-20808, 1419730, Feb. 2018. doi: 10.2172/1419730.
- [6] R. E. MacFarlane and A. C. Kahler, "Methods for Processing ENDF/B-VII with NJOY," *Nuclear Data Sheets*, vol. 111, no. 12, pp. 2739–2890, Dec. 2010, doi: 10.1016/j.nds.2010.11.001.
- [7] D. A. Brown *et al.*, "ENDF/B-VIII.0: The 8th Major Release of the Nuclear Reaction Data Library with CIELO-project Cross Sections, New Standards and Thermal Scattering Data," *Nuclear Data Sheets*, vol. 148, pp. 1–142, Feb. 2018, doi: 10.1016/j.nds.2018.02.001.
- [8] JEFF Scientific Co-ordination Group, NEA Data Bank, and NEA Data Bank Member Countries, "JEFF-3.2 evaluated data library - Neutron data," *Nuclear Energy Agency*, Mar. 05, 2014. http://www.oecd-nea.org/dbforms/data/eva/evatapes/jeff_32/ (accessed May 17, 2019).
- [9] A. J. Koning, D. Rochman, J.-Ch. Sublet, N. Dzysiuk, M. Fleming, and S. van der Marck, "TENDL: Complete Nuclear Data Library for Innovative Nuclear Science and Technology," *Nuclear Data Sheets*, vol. 155, pp. 1–55, Jan. 2019, doi: 10.1016/j.nds.2019.01.002.
- [10] J. Meija *et al.*, "Atomic weights of the elements 2013 (IUPAC Technical Report)," *Pure and Applied Chemistry*, vol. 88, no. 3, pp. 265–291, Mar. 2016, doi: 10.1515/pac-2015-0305.
- [11] J. Brookman, "As-Run Physics Analysis for the University of Florida B-1 Project in the ATR," Idaho National Laboratory, Idaho Falls, ID, INL Engineering Calculations and Analysis 3193–0, Mar. 2016.
- [12] "Math.NET Numerics." <https://numerics.mathdotnet.com/> (accessed Feb. 18, 2020).
- [13] dotnet-bot, "Complex Struct (System.Numerics)." <https://docs.microsoft.com/en-us/dotnet/api/system.numerics.complex> (accessed Feb. 18, 2020).
- [14] B. T. Rearden *et al.*, "OVERVIEW OF SCALE 6.2," OSTI Report 1095656, 2013. [Online]. Available: <https://www.osti.gov/biblio/1095656>.
- [15] G. van Rossum, "Python tutorial," Centrum voor Wiskunde en Informatica, Amsterdam, the Netherlands, CS-R9526, 1995. [Online]. Available: <https://ir.cwi.nl/pub/5007/05007D.pdf>.

Appendix A: Select Enlarged Figures

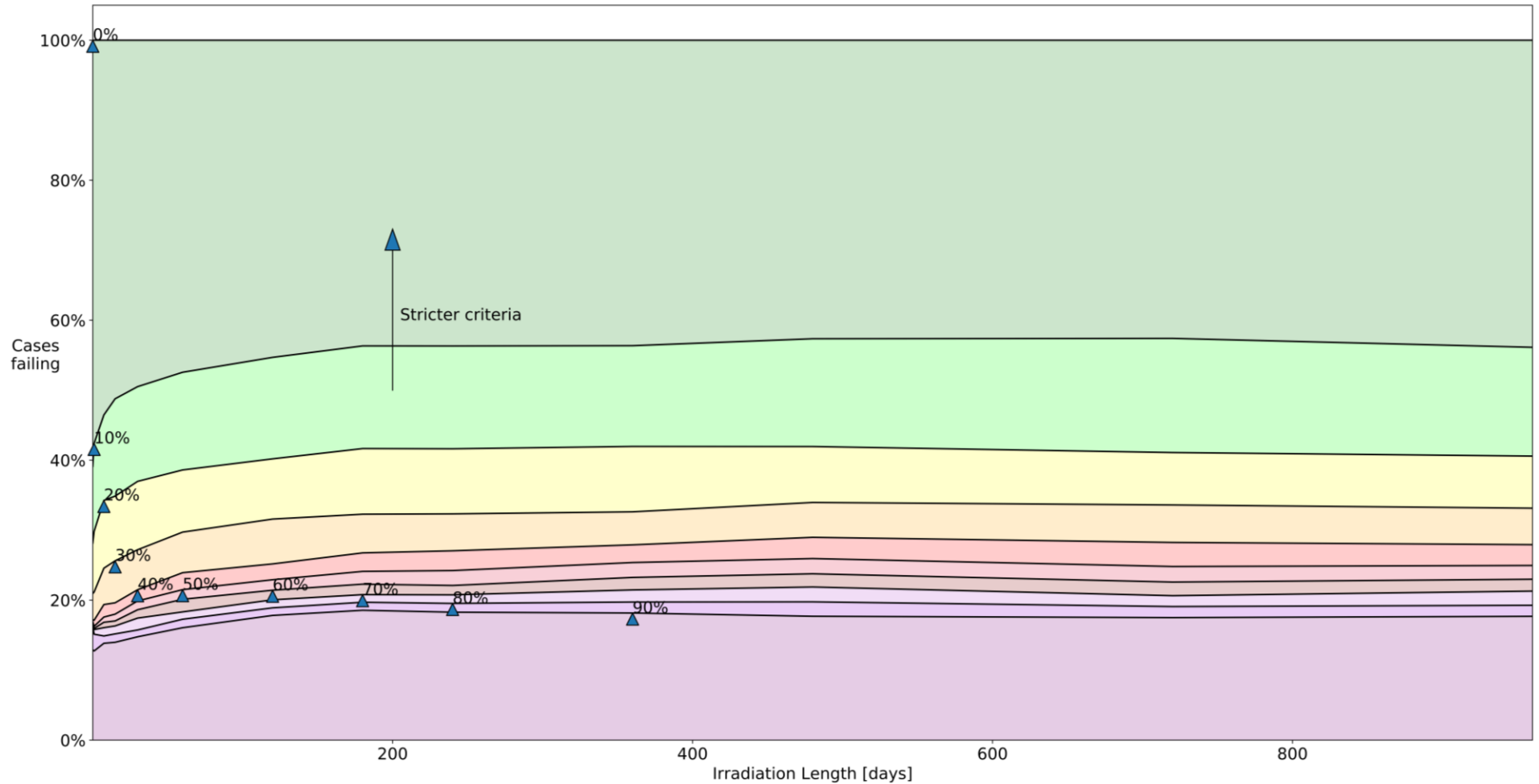


Figure 9. Accuracy of the RAD calculator when compared to ORIGEN based on simulated irradiation length. Each color band represents a range of absolute percent differences between the RAD calculator and ORIGEN. The y-axis is the proportion of cases failing within these various tolerance bands. A high-pass filter of 0.1 mrem/hr/g for the ORIGEN test case was applied to remove the effects of different cutoff thresholds.

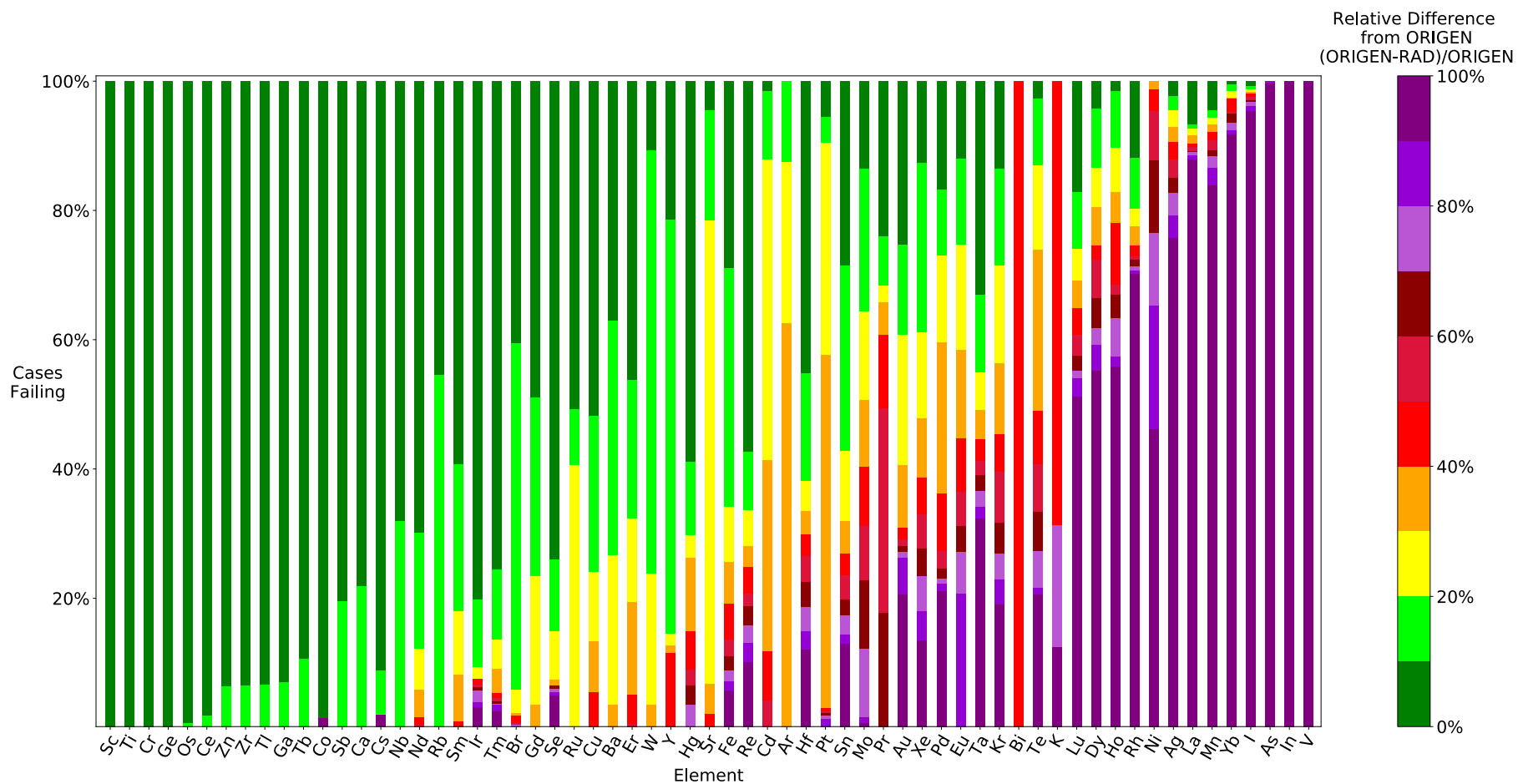


Figure 10 The accuracy of the RAD calculator compared to ORIGEN for specific gamma dose rate with respect to the simulated element irradiated. Each color band represents a range absolute percent differences between the RAD calculator and ORIGEN. The y-axis is the number of cases falling within these various tolerance bands. A high pass filter of 0.1 mrem/hr/g for the ORIGEN test case was applied to remove the effects of different cutoff thresholds.

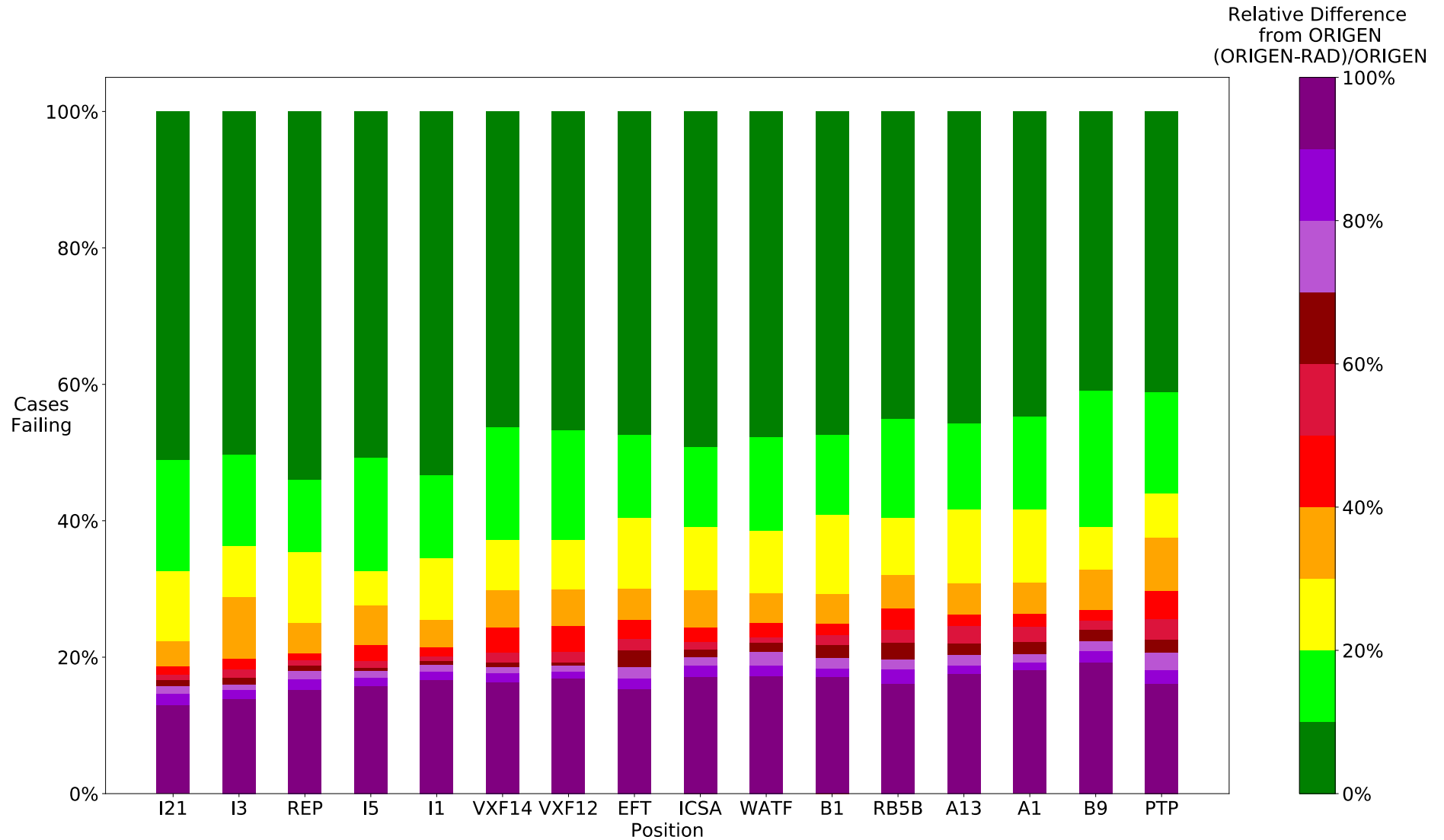


Figure 11. Accuracy of the RAD calculator compared to ORIGEN for specific gamma dose rate with respect to the reactor position used. Each color band represents a range of absolute percent differences between the RAD calculator and ORIGEN. The y-axis is the number of cases falling within these various tolerance bands. A high-pass filter of 0.1 mrem/hr/g for the ORIGEN test case was applied to remove the effects of different cutoff thresholds.

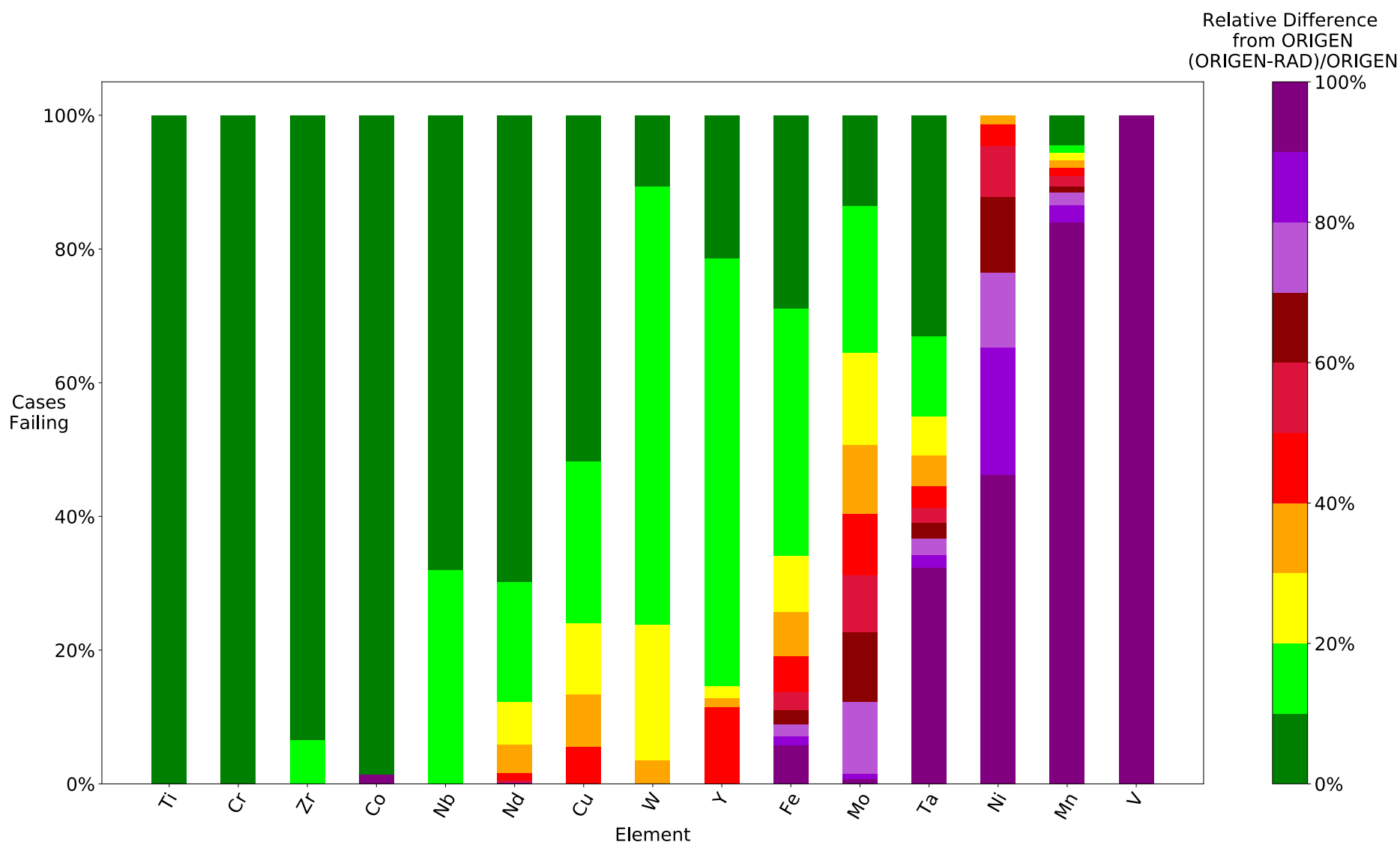


Figure 12. Accuracy of the RAD calculator, as compared to ORIGEN, for specific gamma dose rate with respect to the simulated element irradiated. Only materials in the NFML are included. Each color band represents a range of absolute percent differences between the RAD calculator and ORIGEN. The y-axis is the number of cases falling within these various tolerance bands. A high-pass filter of 0.1 mrem/hr/g for the ORIGEN test case was applied to remove the effects of different cutoff thresholds.

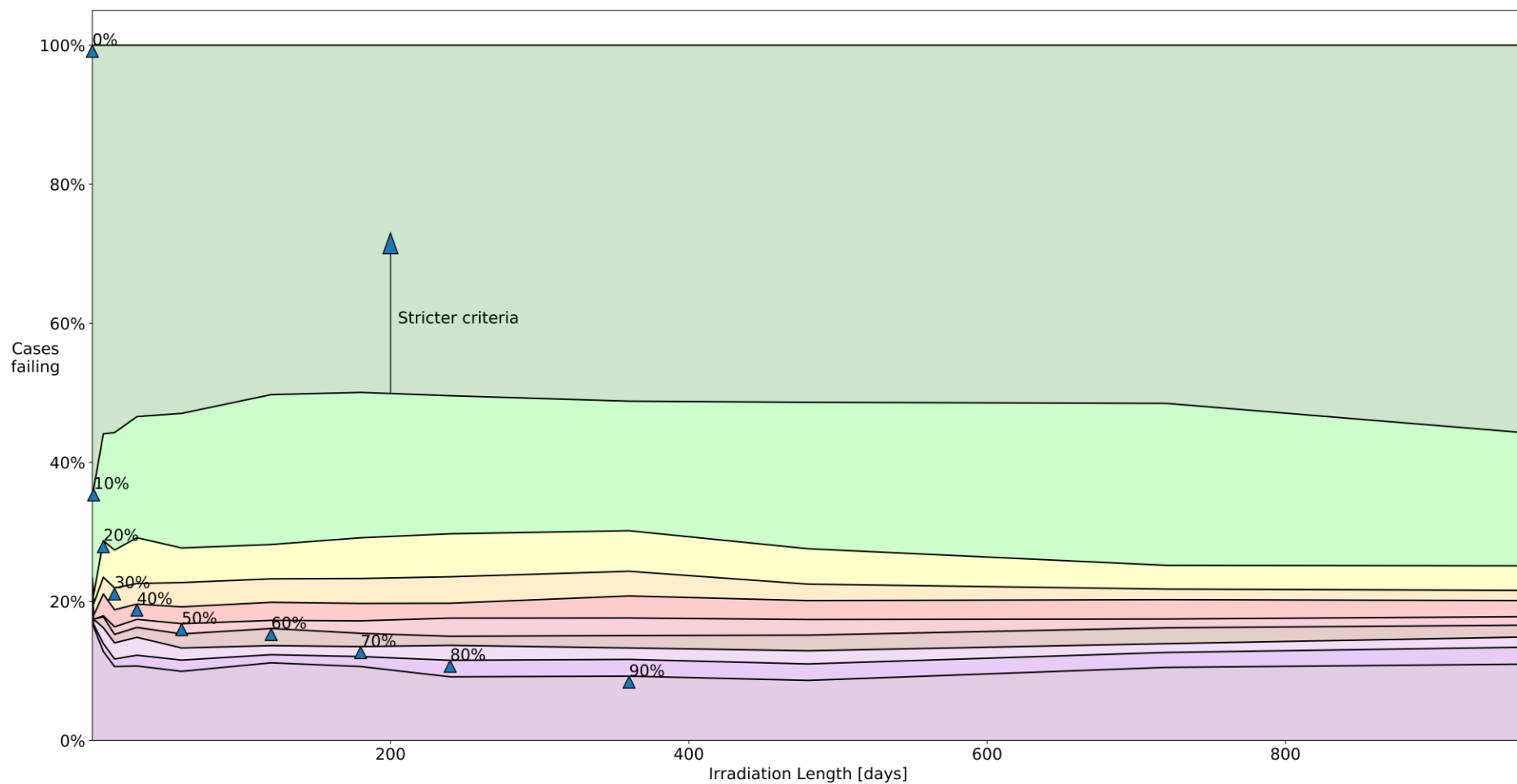


Figure 13. Accuracy of the RAD calculator, as compared to ORIGEN, for specific gamma dose rate with respect to the simulated irradiation length. Only materials in the NFML are included. Each color band represents a range of absolute percent differences between the RAD calculator and ORIGEN. The y-axis is the number of cases falling within these various tolerance bands. A high-pass filter of 0.1 mrem/hr/g for the ORIGEN test case was applied to remove the effects of different cutoff thresholds

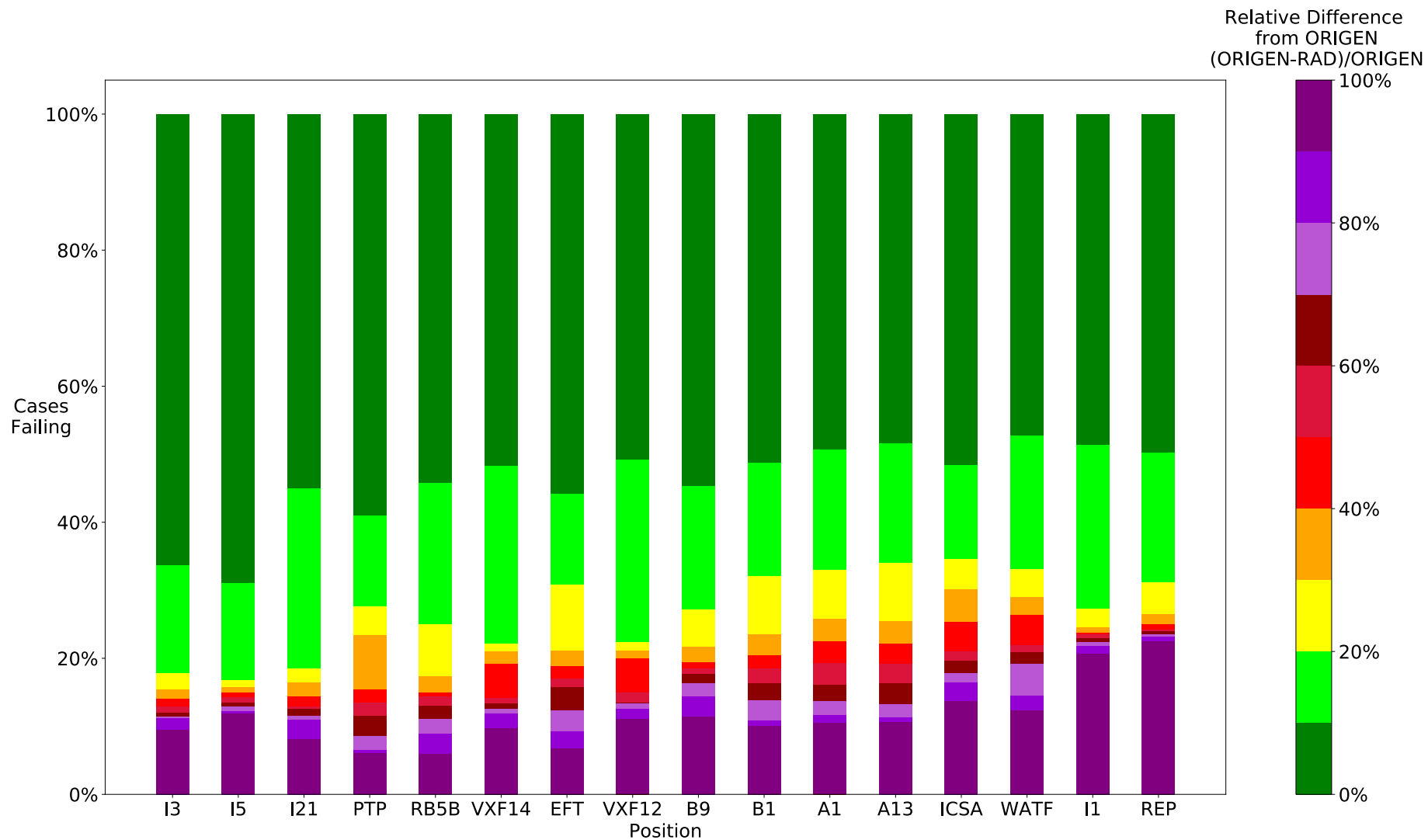


Figure 14. Accuracy of the RAD calculator, as compared to ORIGEN, for specific gamma dose rate with respect to the reactor position used. Only materials in the NFML are included. Each color band represents a range of absolute percent differences between the RAD calculator and ORIGEN. The y-axis is the number of cases falling within these various tolerance bands. A high-pass filter of 0.1 mrem/hr/g for the ORIGEN test case was applied to remove the effects of different cutoff thresholds.

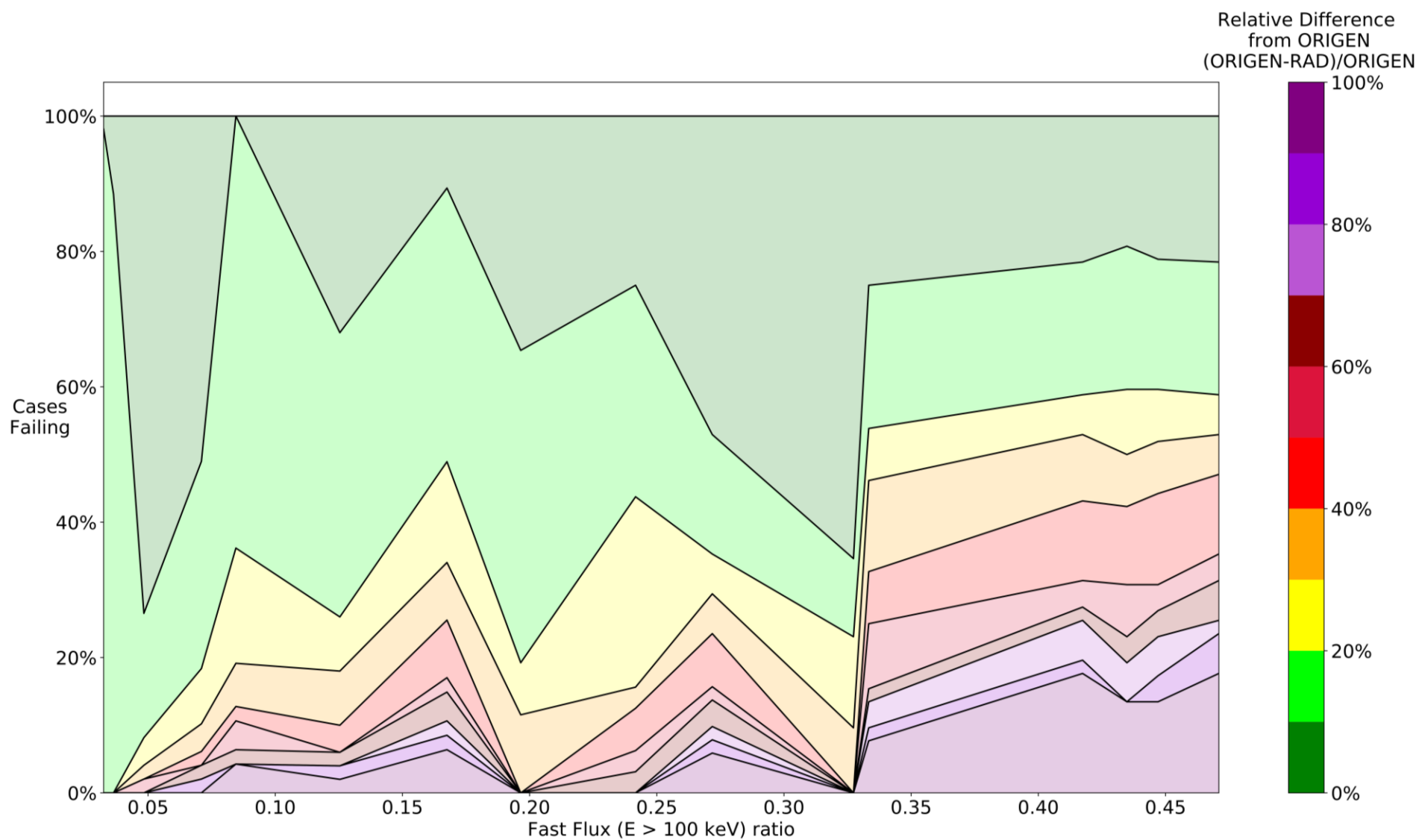


Figure 15. Accuracy of the RAD calculator, as compared to ORIGEN, for specific gamma dose rate for iron with respect to the fast-to-total-flux ratio for each reactor position. For this case, the fast flux cutoff is 100 keV. Each color band represents a range of absolute percent differences between the RAD calculator and ORIGEN. The y-axis is the number of cases falling within these various tolerance bands. A high-pass filter of 0.1 mrem/hr/g for the ORIGEN test case was applied to remove the effects of different cutoff thresholds.